

## Coupling spatially distributed river and groundwater transport models to investigate contaminant dynamics at river corridor scales

Diogo Costa <sup>a, b, \*</sup>, Paolo Burlando <sup>c</sup>, Shie-Yui Liong <sup>b</sup>

<sup>a</sup> Singapore-ETH Centre for Global Environmental Sustainability, Future Cities Laboratory, Singapore

<sup>b</sup> Department of Civil and Environmental Engineering, National University of Singapore, Singapore

<sup>c</sup> Institute of Environmental Engineering, ETH-Zürich, Switzerland



### ARTICLE INFO

#### Article history:

Received 17 November 2015

Received in revised form

8 September 2016

Accepted 10 September 2016

Available online 28 September 2016

#### Keywords:

River-groundwater systems

Fully coupled models

Contaminant transport

Water quality

River reach and corridor scales

### ABSTRACT

Rivers and aquifers are mutually dependent components of the hydrological cycle, typically characterised by temporal dynamics that are a few orders of magnitude apart. This characteristic is often advocated to justify the use of independent single-system models to maximise the outcome for the available computational resources. However, the rapid increase in computational power presently provides means to explore new and more complex modelling schemes, which better reflect the complex physical reality. We present a new modelling framework, FLUXOS, developed from the full coupling of modified versions of state-of-the-art standalone river and groundwater flow and transport models. The model is validated against analytical solutions and applied to real world scenarios in the complex urban corridor of the Ciliwung River in Jakarta to show its flexibility for practical applications and its capabilities as an exploratory tool for realistic investigation of contamination sources and pathways determining non-linear behaviours of river-aquifer interactions.

© 2016 Elsevier Ltd. All rights reserved.

### Software availability

Program name: FLUXOS

Developer: Diogo Costa

Contact address: Singapore-ETH Centre for Global Environmental Sustainability, Future Cities Laboratory, 1 CREATE Way, #06-01 CREATE Tower, Singapore 138602, Tel: +65 6601 4053, E-mail:[pinfo.da.costa@arch.ethz.ch](mailto:pinfo.da.costa@arch.ethz.ch)

Year first available: 2016

Program language: Fortran 90 and Fortran 77

Software requirements: MS Windows, libicoremd.dll, libiomp5md.dll, libmmd.dll and msvr100d.dll

Software development: MS Visual Studio 2010, Intel(R) Visual Fortran Composer XE 2011, or above, and Intel(R) Fortran Compiler XE 12.0

Software availability: contact the authors

Web page: <http://www.fcl.ethz.ch>

### 1. Introduction

Half of the world's population lives in cities and the number is still rising. Particularly in developing countries, many urban areas are rapidly sprawling into sizable megacities ([Zipperer and Pickett, 2012](#)) without developing adequate sanitary infrastructures. By 2050 the number of people residing inside urban perimeters is expected to reach 70% ([Heilig, 2012](#)), turning the conservation of water resources and the protection of human and ecological health from increasingly polluted rivers into a foremost challenge.

Solid waste and widespread water pollution are currently major sources of contamination of many urban rivers ([Un-Habitat, 2008](#)). Urban runoffs, which often carry high levels of heavy metals originating from road traffic, are now becoming also increasingly rich in pathogens and organic substances ([Zoppou, 2001](#)) because of the imbalance between growth of spontaneous settlements and construction of infrastructures.

Urban pollution is visibly affecting the quality of water in many rivers around the world. Moreover, numerous studies have shown over the years that contamination is reaching the underlying groundwater resources despite the highly impermeable surfaces of urban areas. Cases of contamination of urban groundwater by sewage leakage from damaged sewers and infiltration of polluted

\* Corresponding author. Singapore-ETH Centre for Global Environmental Sustainability, Future Cities Laboratory, Singapore.

E-mail addresses: [pinfo.da.costa@arch.ethz.ch](mailto:pinfo.da.costa@arch.ethz.ch) (D. Costa), [paolo.burlando@ifubaug.ethz.ch](mailto:paolo.burlando@ifubaug.ethz.ch) (P. Burlando), [tmsly@nus.edu.sg](mailto:tmsly@nus.edu.sg) (S.-Y. Liang).

river waters are commonly found in the literature (e.g., Lerner, 2002).

In many cases, the problem is further aggravated by increased interaction between shallow and deeper aquifers due to excessive pumping, which favours the propagation and/or migration of contamination across different layers in the groundwater system.

Finally, evidences of an increase in the frequency of flooding has been observed in many regions around the globe (Hallegatte et al., 2013) and attributed to different phenomena, thereby including climate change, reduced permeability and increased encroachment of river margins. In some cases, such changes affect the hydraulic regime of rivers, which in turn, significantly reverberates in the river-aquifer dynamics and has been linked to pollution problems (e.g., Wong et al., 2010).

The number of urban areas, where pollution, flooding, excessive pumping and dependency on groundwater emerge as phenomena that induce more complex interaction across water bodies, is continuously rising, thus requiring a more integrated approach to rivers-aquifers systems management.

Accordingly, determining the circumstances which can generate flow and transport dynamics across river and aquifer systems leading to critical pollution states (e.g., Rassam et al., 2008) is extremely important. Unfortunately such processes are yet poorly understood and there is a lack of appropriate modelling tools to address river-aquifer interaction, particularly in urban environments and for cases involving unsteady contaminant exchange. This is best addressed by the joint simulation of flow and transport processes across the river-aquifer boundary (Rassam, 2011), as done by the modelling framework presented in this article.

## 2. State-of-the-art

It is well known that rivers and groundwater exchange flow and mass at rates that vary over space and time (e.g. Tian et al., 2015; Kalbus et al., 2006). These fluxes depend on the hydraulic and water quality characteristics at the interface (Winter, 1999). These are dynamic and can determine conditions, which lead to exchange patterns that are non-linear (Sophocleous, 2002).

To capture these phenomena, hydrological models coupling surface water (SW) and groundwater (GW) components have emerged with the purpose of investigating the hydrology of river basins thereby including SW-GW systems at catchment scales. Some popular models belonging to this category are MODHMS (Loague et al., 2006), InHM and HydroGeoSphere (Brunner and Simmons, 2012), MIKE-SHE (Refsgaard et al., 1995; Ma et al., 2016) and tRIBS (Ivanov et al., 2004). However, while the target scale of these models (watersheds) allows for the diffusion wave assumption or other simplified overland flow routing methods, for river reach and corridor scale studies such simplifications are unsuitable, especially to simulate phenomena such as flooding and turbulence, and the associated transport processes, which require a greater level of detail.

Models coupling surface unsteady hydrodynamic and groundwater flow solvers started emerging little more than 10 years ago when computers became increasingly faster and more efficient (e.g. Shaad, 2015). Examples of these models are SWIFT2D-SEAWAT (Langevin et al., 2005), MODFLOW-LGR-VSF-newCFL (Borsi et al., 2013), MODFLOW-OWHM (Hanson et al., 2014) and 2dMb-MODFLOW (Ruf, 2007; Shaad, 2015).

However, the full coupling of 2-dimensional surface and 3-dimensional groundwater flow models is still incipient (Furman, 2008), e.g. not many of the models allow for moving boundary problems for flooding and wetland studies, and the further integration of transport and water quality subroutines is largely unexplored (e.g. Zerihun et al., 2005).

A wide range of popular surface and groundwater models, which can generally simulate either river or aquifer dynamics only, are currently available. However they are not suitable for detailed river-aquifer flow and mass flux estimations in complex cases involving transient conditions and/or in irregularly-shaped streambeds due to a number of reasons, namely:

1. Most are single-system models developed to address typical river (e.g., QUAL2E, Brown and Barnwell, 1987) or aquifer (e.g., PHT3D, Prommer et al., 2003) problems. While processes affecting the targeted systems are explicitly modelled, those arising from interactions with the other, non-modelled systems are, if included at all, forced through a set of boundary conditions, the definition of which is in many cases simplified or difficult to link with reality (see Fig. 1).
2. The interaction between river and aquifer in both the channel and the floodplain is a complex and dynamic process. It may occur in both directions, depending on the relative position of the water table and the river water level. Flow and mass exchange between river and aquifer are however often ignored or simplified to uniform or linearly-varying predefined rates (e.g., MT3DMS and MODFLOW; Zheng and Wang, 1999; Harbaugh et al., 2000).
3. Thus, reversing the direction of the fluxes across the interface may occur, in turn causing each system to act alternatively as source or sink (see Fig. 2).

Therefore, a realistic simulation of the exchange of mass through the river-aquifer interface, which depends on the continuously changing pressure gradients and distribution of concentrations across the system acting as a source, which may change over time, requires solving river and groundwater flow and transport equations in parallel, alongside with explicit tracking of interactions and continuous update of the surface and groundwater systems. In the case of externally coupled river and groundwater models, such flux oscillations caused by river-aquifer interdependent dynamics are not simulated and are typically forced through boundary conditions.

4. Externally coupled flow and transport models have additionally the disadvantage that flow information needs to be stored by the flow model for subsequent use by the transport subroutine/model. This may lead to a disproportionate growth of storage needs during long term simulations, thus making external coupling unattractive or sometimes impossible.

An example of a fully coupled model attempting to solve the limitations enumerated above is provided by the coupling of MIKE FLOOD – a 1D/2D surface hydrodynamic model – to FEFLOW – a 2D/3D groundwater flow, transport and water quality finite element model. The coupling makes use of MIKE11 – the 1D hydrodynamic solver of the river network in MIKE FLOOD – through the *ifmMIKE11* plug-in, which allows both models to exchange flow and mass information at all time steps, thus allowing the coupled model to mimic a possible exchange of flow and transport direction during transient conditions. However, the interaction between river and aquifer is limited to the pre-defined river network, due to the 1D character of the surface hydrodynamic model, thus making impossible the simulation of inundation events, which extend over the broader river corridor.

Another model worth to mention is the control-volume finite element hydrological model HydroGeoSphere (HGS), which aims at simulating the terrestrial portion of the hydrological cycle. It is a fully-integrated subsurface and surface flow and solute transport that solves the 2D diffusion wave equation. This is appropriate for

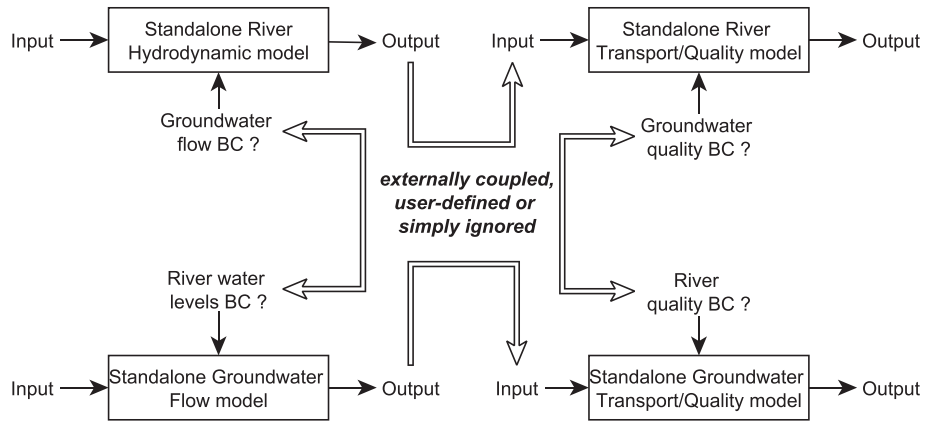


**Fig. 1.** Conventional scheme of external coupling of standalone models. BC refers to boundary conditions. One-way simulation paths do not allow accounting for feedback processes occurring between systems.

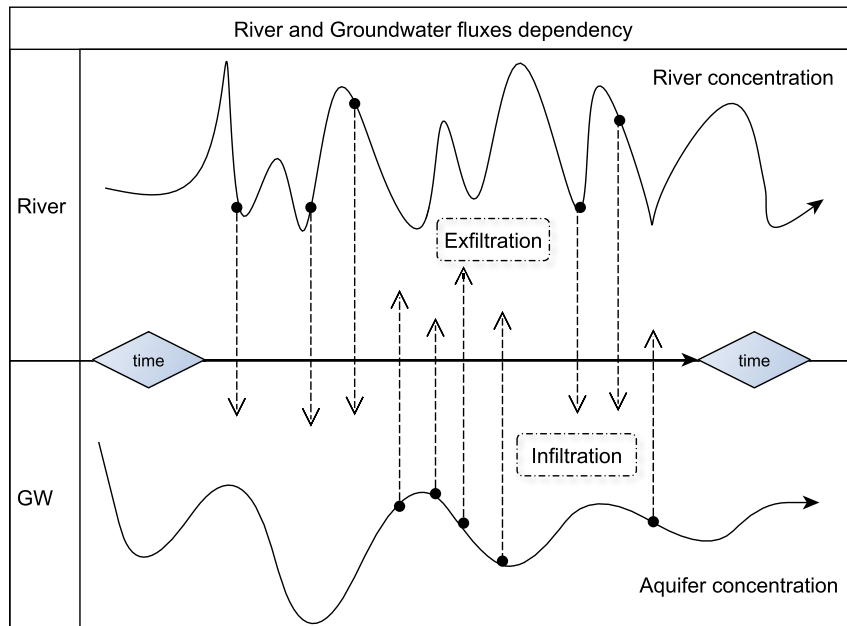


**Fig. 2.** River-groundwater mass exchange feedback is highly variable. The vertical arrows show the hypothetical direction of a mass transfer, the magnitude and the nature of which depends on the concentration distribution of the system acting as a source, respectively the river in the case of infiltration and the aquifer in the case of exfiltration, and on conditions that may induce non-linear behaviours.

gradually varying flow in mild slopes but less suitable to investigate unsteady flow regimes involving flood propagation in complex irregular streambeds.

Although joint modelling of 2D surface and 3D groundwater flow combined with transport and water quality simulation is typically computationally demanding, the computational price to pay is worth the gain of an unparalleled ability to explore integrated river-aquifer pollution problems, especially considering the challenges posed by the complexity of interactions in environments like the urban and peri-urban river corridors for both diagnostic and planning purposes.

In this context, this article discusses the technical and numerical challenges of the internal coupling of 2D surface and 3D groundwater reactive-transport solvers to an integrated river-aquifer flow model by introducing a novel process based modelling framework – named as FLUXOS – that is a considerable step forward in

overcoming the limitations of compartmented modelling, while being suitable to address real world problems. Early applications of the tool presented here and documented in Costa et al. (2015, 2016a,b) showed that it can effectively help revealing mechanisms from limited measurements and allows for more integrated river-aquifer exploratory analysis. This article reinforces those conclusions by showing additional applications, which further demonstrate the potential of the novel model. Such potential is of great use for more effective and forward-looking pollution control in large cities. In this respect, this article focuses primarily on the development, testing and validation of the coupled model, as well as on discussing, through integrated modelling examples, its flexibility to investigate pollution problems in urban areas, which may go beyond those contemplated in the referred early exploratory applications.

### 3. Model and software design

#### 3.1. Software architecture

The novel modelling framework, FLUXOS, explicitly couples two state-of-the art transport models – one for surface water (+QeS2, Costa et al., 2014) and one for groundwater (MT3DMS, Zheng and Wang, 1999) – to an integrated river-aquifer flow model (2dMb+MODFLOW-2005, Shaad, 2015).

These models were modified to be integrated into FLUXOS as model components/subroutines that are controlled and internally coupled through a main program. This rules the simultaneous solution of flow and transport equations and also computes the exchange fluxes of water and tracers, across the continuum of river and groundwater systems. Fig. 3 shows a simplified representation of the modelling framework architecture and of the simulated processes, whereas Fig. 4 shows a simplified flowchart of the main program that rules the explicit coupling of the single model components.

The surface hydrodynamic and transport model components – respectively a modified version of 2dMb (Shaad, 2015; Fäh, 1997) and +QeS2 (Costa et al., 2014; Fäh, 1997) – solve the 2D depth-averaged shallow water and the transport partial differential equations (PDEs) in the two-dimensional (2D) Euclidean space. There is no need to specify the location of the streams as the discretization of the topography is used to capture surface flow and transport dynamics across the river corridor domain. The two groundwater model components – respectively a modified version of MODFLOW and MT3DMS – solve the 2D/3D groundwater flow and transport PDEs (see the manual of the standalone model versions in Harbaugh (2005); Zheng and Wang (1999), respectively).

While 2dMb and MODFLOW models have been modified, coupled and validated by Shaad (2015), the modification and further coupling of both +QeS2 and MT3DMS models as subroutines of the new coupled model are the main objectives of this work.

Some important characteristics of the coupled 2dMb-MODFLOW model, which were used as the basis for the development of FLUXOS include (1) the use of a 2D interface layer as a central drive for the mapping of the information (i.e. flow and hydraulic

pressure), which is exchanged at each time step between the surface and subsurface model components to minimise the need for major changes in the solvers of the original model components; (2) the use of source/sink terms in all flow and transport equations of both surface and subsurface domains to account for the effect of the interaction fluxes between the two systems, which is computed using the conductance-based model at the interface layer; and (3) the grid mapping of corresponding (i.e. contiguous) cells in the surface and subsurface domains (as an input file) prior to the simulation for the computation of the vertical exchange fluxes.

The time step used in each flow model component is independently calculated and continuously updated throughout the simulation to obey the Courant (CFL) condition (Courant et al., 1928). Similarly, the transport components obey the Péclet condition (Carey and Pardhanani, 1989).

The time steps required by the groundwater models – typically hours or days – can be as much as  $\approx 10^4$  times higher than those in the river models, which are typically of the order of seconds or tenth of seconds depending on the grid resolution and flow conditions. These differences are managed through the sequence in which the main program calls each model component and runs through inner loops.

#### 3.2. Modifying and coupling model components

The standalone original versions of all model components required changes to make possible their integration into a fully coupled framework. In particular, time loops have been deactivated and the code recompiled as subroutines of the main program.

Since the main programs 2dMb and +QeS2 are written in FORTRAN 90 but MODFLOW and MT3DMS in FORTRAN 77 and 90/95, the latter were modified to be recompiled into DLL (Dynamic Link Library) so that they can be shared across the new model framework without changing their original program languages. This aims at making easier the update of any model component in the future from new versions of the original standalone source codes.

MT3DMS was modified to run in parallel to MODFLOW, hence both the MODFLOW package *Link-MT3DMS*, which stores flow information to be read by MT3DMS, and the MT3DMS *Flow Model*

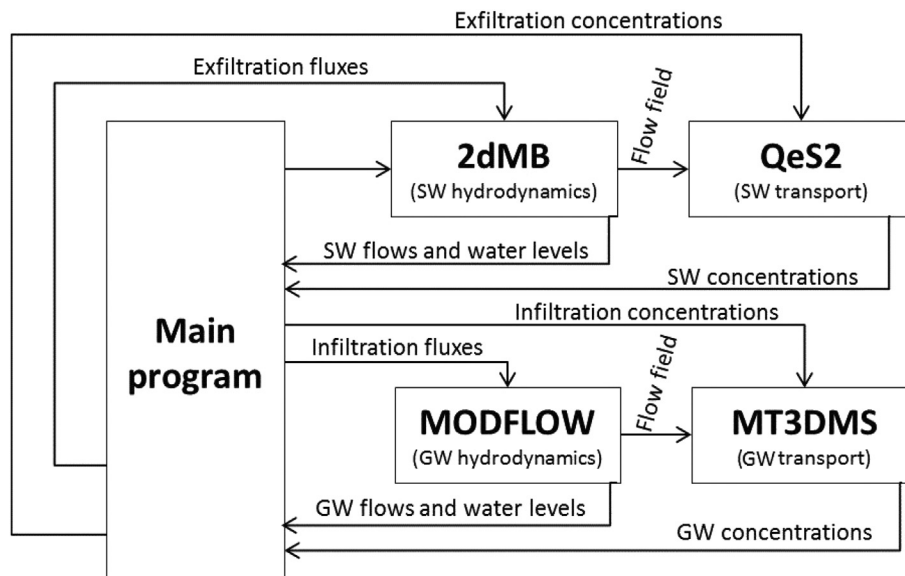


**Fig. 3.** Simplified representation of the architecture of the coupled modelling framework.

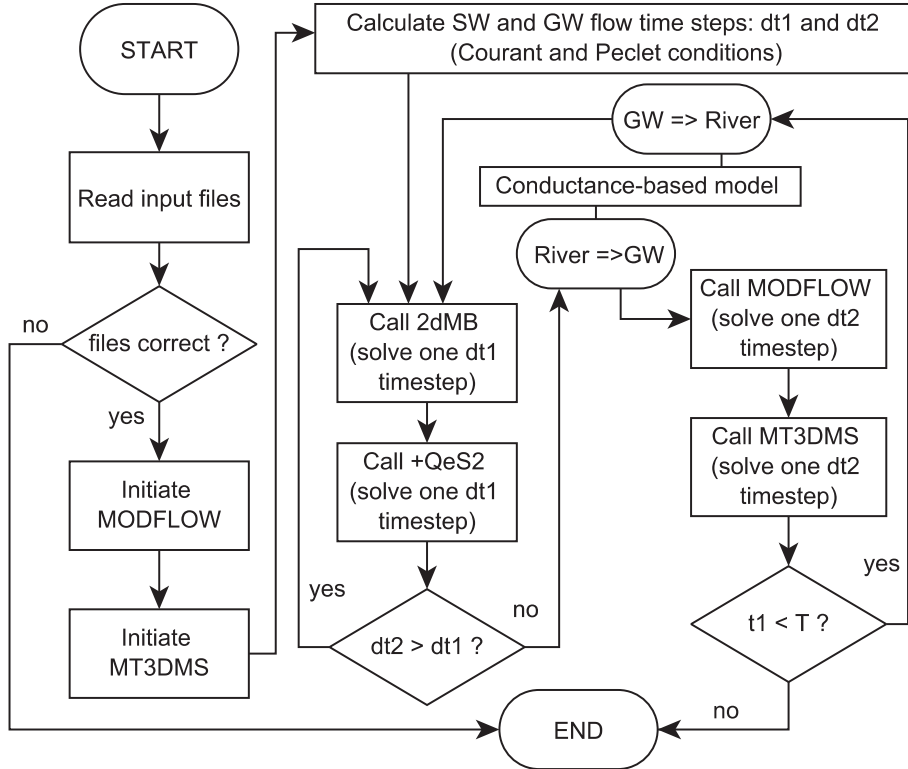


**Fig. 4.** Flowchart of the main program. T denotes the simulation period and  $dt_1$  and  $dt_2$  are the flow time steps calculated obeying the Courant condition for the SW and GW domains respectively.

*Interface Package-FMI350*, which in turn reads the stored flow information, were both deactivated. MODFLOW was accordingly modified to directly communicate with the modified version of MT3DMS by means of internal, i.e. through the main program, bypassing of flow information at every time step.

All functionalities of the original surface and groundwater flow models versions (e.g. *Well and General-Head boundary* packages in MODFLOW) have been included in the modified versions by Shaad (2015) and are supported by the coupled framework.

Similarly, all functionalities of the original versions of the transport components (e.g. *Dispersion and Sink & Source Mixing* packages in MT3DMS) were modified to be compatible with the new model architecture.

The Cartesian coordinate system characterising each of the original models remains unchanged in the coupled framework. Although the convention used to discretise the physical domain in the standalone versions of 2dMb and +QeS2 differs from that used in both MODFLOW and MT3DMS, both conventions are maintained in all modified model versions, but are harmonized in the main program through a set of algebraic operations performed using information about river to groundwater cell correspondence – panel (a), Fig. 5. This strategy was initially adopted in 2dMb+MODFLOW integrated model (Shaad, 2015), and is now extended to the transport model components.

To improve computational efficiency, the surface water and groundwater components are allowed to run at different grid-size and time step resolutions. In the case of different river and groundwater grid-sizes (panel (b), Fig. 5), the information exchanged across the two models is reconciled by the main program through a set of algebraic operations, such as shown in Eq. (1a) and (1b) for respectively the exfiltration (E) and infiltration (I) cases.

$$E(s_{i,j}) = E(s_{i+1,1}) = E(s_{i,j+1}) = \dots = E(g_{k,l}) / n \quad (1a)$$

$$I(g_{1,ny}) = I(s_{i,j}) + I(s_{i+1,1}) + I(s_{i,j+1}) + I(s_{i+1,j+1}) + \dots \quad (1b)$$

where n is the number of SW cells in each GW cell.

When river and aquifer model components run at different time steps, which is also frequently the case, the main program handles the order and sequence in which each model component is activated, such as depicted in Fig. 4. But it also integrates results from the models running at smaller time steps, be it flow or transport related, to transfer their outcomes, when called, to the models running at larger time steps.

The effect of the exchange of contaminants between the surface and subsurface domains is introduced by means of a source term added to the reactive-transport equations solved by each of the corresponding model components.

In the case of the modified +QeS2 model component, we have thus

$$\frac{\partial \xi c_s}{\partial t} + \frac{\partial \xi u c_s}{\partial x} + \frac{\partial \xi v c_s}{\partial y} - \frac{\partial}{\partial x} \left( \xi E_x \frac{\partial c_s}{\partial x} \right) - \frac{\partial}{\partial y} \left( \xi E_y \frac{\partial c_s}{\partial y} \right) + S = 0, \quad (2)$$

where  $c_s$  is the concentration of a dissolved substance in the surface water [ $ML^{-3}$ ];  $E$  is the horizontal diffusivity [ $L^2T^{-1}$ ]; and  $S$  is a source term [ $ML^{-2}T^{-1}$ ].

In the case of the modified MT3DMS model component, we have

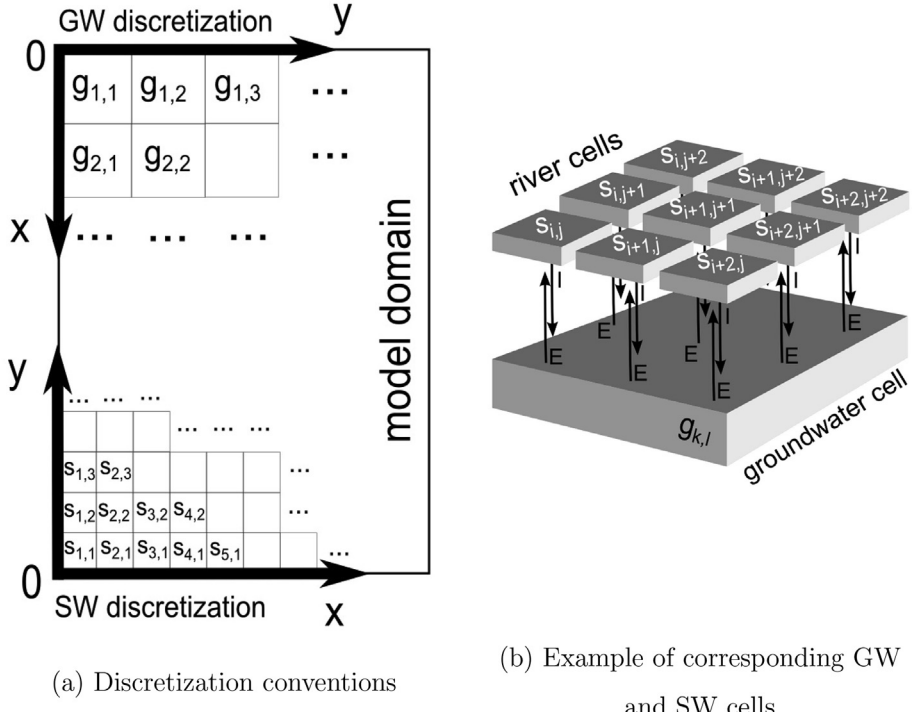


**Fig. 5.** (a) Cell discretization in both the SW and GW model components. (b) Example of corresponding SW and GW cells where I and E represent infiltration and exfiltration fluxes.

$$\begin{aligned} \frac{\partial \theta c_g}{\partial t} + \frac{\partial}{\partial x} (\theta v_x c_g) + \frac{\partial}{\partial y} (\theta v_y c_g) + \frac{\partial}{\partial z} (\theta v_z c_g) - \frac{\partial}{\partial x} \left( \theta D_x \frac{\partial c_g}{\partial x} \right) \\ - \frac{\partial}{\partial y} \left( \theta D_y \frac{\partial c_g}{\partial y} \right) - \frac{\partial}{\partial z} \left( \theta D_z \frac{\partial c_g}{\partial z} \right) - q_s c - \sum R_n = 0, \end{aligned} \quad (3)$$

where  $c_g$  is the concentration of a dissolved substance in the groundwater [ $\text{ML}^{-3}$ ],  $\theta$  is the porosity of the porous material [–],  $v_i$  is the linear pore water velocity which is given by  $v_i = q_i/\theta$  [ $\text{LT}^{-1}$ ];  $q_s$  is a volumetric flow rate per unit volume [ $\text{T}^{-1}$ ];  $\sum R_n$  is a chemical reaction term [ $\text{ML}^{-3}\text{T}^{-1}$ ]; and  $D_i$  is the dispersion coefficient [ $\text{L}^2\text{T}^{-1}$ ] calculated from dispersivity (Burnett and Frind, 1987) as e.g.  $D_x = \alpha_L \frac{v_x^2}{|v|} + \alpha_T \frac{v_y^2}{|v|} + \alpha_V \frac{v_z^2}{|v|}$ , where  $\alpha_L, \alpha_T$  and  $\alpha_V$  are the dispersivities in the longitudinal, transverse and vertical directions.

The reader is referred to the Supplementary Material for more information about the governing equations solved by each of the model components integrated in FLUXOS, as well as the implemented mathematical transformations.

### 3.3. Pollution loading schemes

The original version of MT3DMS has a *Sink and Source Mixing Package*, which allows associating pollution schemes to selected MODFLOW packages, such as the *Well Package* or the *Drain Package*. Conversely, +QeS2 was developed on the basis of an existing subroutine of 2dMb used for sediment transport simulations, which was replicated in the form of a number of auxiliary subroutines that allow the concomitant simulation of different river pollution source types. These account for two different types of sources, namely point and distributed.

The first type includes instantaneous point sources to simulate spill-type loadings and continuous point sources to mimic outlet-type loadings. In the latter, a linear-ramp algorithm scheme was

included as it can be conveniently used to approximate almost any loading pattern (e.g. diurnal variation of discharges in domestic outlets) through successive linear approximations. The instantaneous and continuous point sources are described respectively by the following equations:

$$dc_{sw} = \begin{cases} M/V_{cell} & \text{if } t = t_i \\ 0 & \text{if } t \neq t_i \end{cases} \quad (4a)$$

$$\frac{dc_{sw}}{dt} = \begin{cases} \frac{dM}{dt}/V_{cell} & \text{if } t_1 < t < t_2 \\ 0 & \text{if } t_1 > t \text{ or } t > t_2, \end{cases} \quad (4b)$$

where  $c_{sw}$  is the concentration of a given tracer in the river,  $M$  is the loading mass,  $t_i$  is the moment at which the instantaneous loading is applied,  $t_1$  and  $t_2$  are the instants between which the mass loading varies, and  $V_{cell}$  is the volume of water in the cell.

Similar loading algorithms are common across many water quality models (e.g. Chapra, 2008) in order to approximate real world pollution sources.

The second family of algorithms accounts for spatially distributed input and includes a uniform and a special build-up/wash-off scheme.

#### The uniform scheme

$$\frac{dc_{sw}}{dt} = K_m/V_{cell}, \quad (5)$$

where  $K_m$  is a loading rate, is relatively common and is most suitable to simulate processes like sediment oxygen demand or reaeration which are dependent on the mobile riverbed characteristics or free-surface area.

The build-up/wash-off loading algorithm was designed to simulate the build-up and wash-off of pollutants on impervious areas, as they typically occur in urban areas, when rivers flood

them. Pollution due to river flooding is an important component of FLUXOS since flood waves are known to transport significant amounts of pollution originating from a number of sources such as roads, sewerage systems and drains in urban areas (Zoppou, 2001).

The concept of build-up/wash-off was adapted from catchment and urban storm water models (e.g., Wang et al., 2011), which use empirical relationships to account for these phenomena (e.g. Zoppou, 2001).

In the modified version of +QeS2, the build-up function was approximated to a zero-order function, thus describing a linear accumulation of overland pollution over time, as

$$\frac{dM}{dt} = k, \quad (6)$$

while the wash-off was represented by a function similar to an instantaneous point-source-type scheme, which is activated whenever a cell in the domain turns wet, that is

$$dc_{sw} = \begin{cases} M/V_{cell} & \text{if } h_{ij}^t \neq 0 \wedge h_{ij}^{t-1} = 0 \\ 0 & \text{otherwise} \end{cases} \quad (7)$$

### 3.3.1. River-groundwater interactions: flow and transport

The interaction between surface and groundwater flow models is updated throughout the simulation based on the relative positioning of the water table and the river water level, which determines either infiltration or exfiltration.

The quantification of these fluxes is computed using a one-dimensional conductance-based model, which was implemented by Shaad (2015). In this model the exchange fluxes are proportional to vertical pressure gradients occurring between river water levels and underlying aquifer water tables. This implies that fluxes depend on the difference between the potentiometric head and the river water level in the case of exfiltration (i.e.  $\psi > z_b$ ) and exclusively on the river water depth in the case of infiltration (i.e.  $\psi \leq z_b$ ). Accordingly,

$$q_v = \begin{cases} -\frac{k}{l}(\xi + z_b - \psi); & \text{if } \psi > z_b \\ -\frac{k}{l}\xi; & \text{if } \psi \leq z_b \end{cases}, \quad (8)$$

where  $q_v$  is the vertical river-groundwater exchange flux per unit area and  $k/l$  is the conductance-parameter [ $T^{-1}$ ].

The latter can be treated in different manners. Two formulations were adopted by Shaad (2015), namely the dominant clogging layer formulation (Eq. (9a)) proposed by Harbaugh (2005) and the distinct clogging layer scheme proposed by Mehl and Hill (2010) and modified by Shaad and Burlando (2014):

$$\frac{k}{l} = \frac{k_c}{b} \quad (9a)$$

$$\frac{k}{l} = \left[ \left( \frac{k_c}{b} \right) + \left( \frac{K_{zz}}{B - b} \right) \right]^{-1}, \quad (9b)$$

where  $k_c$  and  $b$  are respectively the hydraulic conductivity and thickness of the conductance layer and  $B$  equals half of the groundwater top layer thickness.

The exchange of soluble material through the hyporheic zone does not depend only on the water fluxes occurring between adjacent river and groundwater (aquifer top) cells, but also on the

concentration distribution in the compartment acting as source. This is computed, prior to calculating the effect of advection and dispersion, by the mass balance equation

$$V_{cell}^{gw} \frac{dc_t^{z=top}}{dt} = q_i s_{t-1} - q_e c_{t-1}^{z=top} \quad (10a)$$

$$V_{cell}^{sw} \frac{ds_t}{dt} = q_e c_{t-1}^{z=top} - q_i s_{t-1}, \quad (10b)$$

where  $q_i$  and  $q_e$  are, respectively, the infiltration and exfiltration fluxes obtained from  $q_v$ , and  $c$  and  $s$  are respectively the concentration in the groundwater and river compartments.

The proposed scheme enables both downward and upward exchange of mass to occur simultaneously in different regions of the domain and to vary throughout the simulation.

Additional information about the governing equations, numerical schemes, input files and other software aspects are provided as [Supplementary Material](#).

## 4. Testing the model performance

The performance of FLUXOS was tested by comparing numerical results with analytical solutions. We focused the tests, and more in general the overall analysis, mainly on the performance of the transport components of FLUXOS since the flow components were investigated and fully documented in Shaad (2015).

### 4.1. Benchmark problem

Due to the absence of proper experimental datasets suitable to test coupled models like FLUXOS, we consider, as benchmark against which we compare the coupled model, the steady state solutions for two separate base-problems, one relevant to river transport model components and the other relevant to the groundwater transport components. Fig. 6 shows the configuration of the systems, which consists of continuous pollution point sources on 2D uniform flow fields. These are located sufficiently far apart to allow the plumes to propagate independently. This allows, in turn, to use analytical solution to validate the +QeS2 and MT3DMS model components of the coupled model as if they were independent.

One limitation in this respect is due to the fact that no analytical solution of the advection-dispersion equation exists for systems with infinite domain extent (see Section 4.2). While assuming domains with no physical limits is reasonable in the context of groundwater, the same does not hold for the case of rivers. We circumvented the problem by defining appropriate boundary conditions, which represent a good approximation of the domain

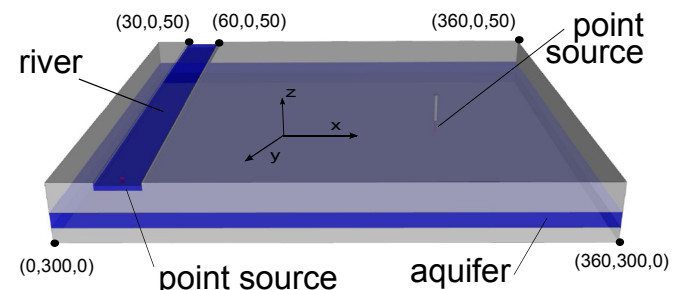


**Fig. 6.** Model domain representation in Cartesian coordinates. It includes a free surface flow region (river) and a groundwater (porous media) slow flow region. Units are in meters.

definition under which the analytical solution is valid. To this purpose, the length of the river was assumed to be infinitely long, to allow advection and dispersion phenomena to develop a transport condition, which can be compared with the analytical solution, before the plume becomes significantly affected by the river banks (i.e. finite river width). Such condition occurs only in the initial phase of the simulation where the propagation of the plume is still largely unaffected by the river width.

The verification of the numerical outputs of FLUXOS is carried out through idealized model configurations and analytical solutions. This is due to the lack of established models that are suitable as benchmark and of analytical solutions of the coupled flow and transport process problem. The model development presented in this paper was indeed motivated by the inability of the existing modelling tools to capture river-aquifer flow and contaminant exchange through a physically-based framework that is suitable for such unsteady simulations of river-aquifer systems that are characteristic of river corridors with irregular channel morphology (e.g. braided systems, frequently inundated floodplains and urban rivers). For example, a verification by comparison with HydroGeoSphere (HGS) would not be meaningful because its surface model components are fundamentally different from those in FLUXOS, particularly the flow component. While HGS solves the diffusion-wave approximation of the Saint Venant equation (neglecting the inertial forces), FLUXOS solves the dynamic-wave which makes it suitable for simulations involving upstream traveling waves often occurring during floods. However, despite the limitations of the verification processes, we consider a critical step to verify that each model component integrated in FLUXOS performs adequately with regards to numerical dispersion, stability and convergence.

#### 4.2. Analytical solutions

Several analytical solutions exist for the unsteady advection-dispersion PDE, which can be applied to both river and groundwater systems. They rely on steady-state and uniform flow conditions and differ mainly for the pollution source scheme, the initial and boundary conditions, as well as for the number of averaged spatial dimensions.

The depth averaged solution for the instantaneous point source problem has been initially proposed by Bear (1979). However, the 2D solution for the continuous point source case, which is obtained from the integration of the point source solution over time, was only partially derived, to the present day, by Wexler (1992) as:

$$c(x, y) = \frac{c_0 Q \exp\left[\frac{V(x-X_c)}{2D_x}\right]}{4n\pi\gamma\sqrt{D_x D_y}} \cdot \int_0^t \frac{1}{t} \exp\left[-\left(\frac{V^2}{4D_x} - \lambda\right)\tau - \frac{(x-X_c)^2}{4D_x\tau}\right. \\ \left. - \frac{(y-Y_c)^2}{4D_y\tau}\right] d\tau, \quad (11)$$

where  $c$  is the concentration of the tracer,  $V$  is the velocity in the  $x$ -direction,  $Q$  is the fluid injection rate,  $n$  is the aquifer porosity,  $X_c$ ,  $Y_c$  and  $Z_c$  are the coordinates of the point source,  $D_x$  and  $D_y$  are the dispersion coefficients in the  $x$  and  $y$  coordinates, and  $\lambda$  is a linear reaction term, which is set to zero for conservative tracers.

The solution is applicable to surface waters by setting the porosity ( $n$ ) equal to one (1). Additional conditions for the derivation of this solution were fluids of constant density and viscosity, advection by uniform flow fields (i.e. constant velocity and water depth) across domains with no physical borders, and Neumann (or

second-type) boundary condition (BC) and initial conditions (IC) respectively described as

$$c, \nabla c = 0, \quad x = \pm\infty; \quad y = \pm\infty \quad (12a)$$

$$c^{t=0} = 0, \quad -\infty < x < \infty; \quad -\infty < y < \infty, \quad (12b)$$

The integral was numerically approximated by means of the recursive adaptive Simpson quadrature method (Gander and Gautschi, 2000) with an accepted absolute error of the order of  $10^{-6}$ .

The solution has a mathematical singularity in the point source region (Abramowitz and Stegun, 2012) because it takes the form of the exponential integral when both  $x - X_c$  and  $y - Y_c$  approach zero, hence becoming infinite at  $\tau = 0$ . However, according to Wexler (1992) the solution is still valid as long as  $(x - X_c)^2$  is larger than  $V^2$ , as it is the case in our simulation domain.

#### 4.3. Model setup and parameterization

**Table 1** summarizes the main characteristics and parameters used in each component of FLUXOS.

The analytical solutions used to test the (transient) transport components requires steady-state and uniform flow fields and given dispersion coefficients. However, the definition of boundary conditions and parameters for both the SW and GW flow components to generate such conditions is not straight forward and requires some additional considerations.

In the case of the GW flow component, the longitudinal pressure gradient ( $dh/dx$ ) and hydraulic conductivity ( $K_x$ ) were defined to produce a seepage velocity ( $v_x$ ) of  $-1/3$  m/s, which was estimated using Darcy's law and directly used in the analytical solution. The resulting specific storage ( $S_s$ ) was calculated as  $2.4 \text{ m}^{-1}$  using  $S_s = K_x \frac{dx}{dt} = K_x v_x$ . The transverse pressure gradient ( $dh/dy$ ) and conductivity ( $K_y$ ) were set, respectively, to zero and  $K_y 10^{-5}$  so that the flow field is unidirectional and along the longitudinal (x-axis) direction (see Fig. 6). The longitudinal and transverse dispersion coefficients used in the analytical solution were calculated from  $D_x \approx \alpha_L v_x$  and  $D_y = \alpha_T v_x$ , where  $\alpha_L$  and  $\alpha_T$  are the dispersivities along the longitudinal and transverse directions (the reader is referred to Fäh (1997) for details on these formulations) as, respectively,  $10/3$  and  $\approx 3/3 \text{ m}^2/\text{day}$ . The initial groundwater potentiometric head was set to vary linearly along the x-axis between fixed heads (eastern and western model boundaries).

In the conductance-based model component, the values proposed in the literature for parameter  $k_c/b$  (conductance over conductance layer thickness) range between 1 and 0.001 m/day (e.g. Brunke, 1999). In this test we used a value of 0.0432 m/day ( $= 5 \cdot 10^{-7} \text{ m/s}$ ), which is representative of a semi-rural area.

To ensure the accurate estimation of flow fields in aquifers subject to infiltration from surface water bodies, the groundwater grid cell resolution should not exceed a characteristic length  $\lambda$  [L] defined as:  $\sqrt{T \cdot c}$ , where  $T$  is the aquifer transmissivity (calculated as  $K_x \cdot H_{aq}$ ) and  $c$  is a resistance term for the interface layer (defined as  $b/K_c$ , where  $b$  and  $K_c$  are, respectively, the thickness and vertical conductivity of the conductance (interface) layer (Haitjema et al., 2001)). The groundwater grid size was fixed to 10 m (see Table 1) which is smaller than the value of  $\lambda$ , calculated as 28.87 m, and therefore compliant with the required condition.

**Table 2** summarizes the initial and boundary conditions and the characteristics of the pollution sources used. For convenience of the validation procedure, two different scenarios, "S1" and "S2", were defined to test, respectively, the SW and GW contaminant transport components and the SW-GW interaction model component.

Scenario "S1" includes two continuous pollution loading points,

**Table 1**

Model setup and parameterization for the testing of FLUXOS.

Model component	Parameters or characteristic	Value	Units
General	domain dimensions (x,y)	360 × 300	m <sup>2</sup>
GW flow	aquifer type	confined	—
	uniform flow field	x-direction	—
	grid size (squared)	10	m
	no. of vertical layers	1	—
	aquifer thickness ( $H_{aq}$ )	10	m
	longitudinal pressure gradient ( $dh/dx$ )	5/360	—
	transverse pressure gradient ( $dh/dy$ )	0	—
	longitudinal hydr. conduct. ( $K_x$ )	7.2	m day <sup>-1</sup>
	transverse hydr. conduct. ( $K_y$ )	$K_x \cdot 10^{-5}$	m day <sup>-1</sup>
GW transport	porosity (n)	0.3	—
	longitudinal dispersivity ( $\alpha_L$ )	10	m
	transverse dispersivity ( $\alpha_T$ )	$0.3\alpha_L$	m
SW flow	IC and BC concentrations	0	mg m <sup>-3</sup>
	grid size	2	m
	CFL threshold	0.4	m
	friction coefficient	0.13	—
	channel slope	0.02	—
	IC: water depth	2	m
	South BC: fixed flow (Q)	50	ms <sup>3</sup>
	North BC: weir	Bernoulli Eq.	—
SW transport	scaling factor for $E_H$ (k)	70.5	—
SW-GW interactions	conductance ( $k_c$ )	0.0432	m day <sup>-1</sup>
	conductance layer thickness (b)	0.5	m

**Table 2**

Characteristics of the initial and boundary conditions and of the pollution sources used. Scenario "S1" is used to testing the individual performance of either the SW and the GW transport components, while scenario "S2" is used to validate the SW-GW interaction model component.

Model component	Parameter	Value		Units
		"S1"	"S2"	
GW transport	point source location (x,y)	270,150	—	m
	point source rate	1000	—	mg day <sup>-1</sup>
SW transport	IC concentrations	0	100	mg m <sup>-3</sup>
	BC concentrations	0	100	mg m <sup>-3</sup>
	point source location (x,y)	44,230	none	m
	point source rate	1000	none	mg s <sup>-1</sup>

one located in the river and one located in the groundwater, to test the performance of, respectively, the SW and the GW transport model components. Scenario "S2", which aims at the testing of the SW-GW interaction model, was forced with only boundary and initial conditions in accordance with the validation method used (see Section 4.1).

Finally, although the flow velocity scalar was set the same for both scenarios, its vector was forced in opposite directions to allow the groundwater plumes to fully develop inside the model domain. Thus, in the case of scenario "S1", the flow moves westwards due to the pollution loading point being located in the eastern part of the domain, whereas in the case of scenario "S2", it moves eastwards because the pollution source, which is the river, is located in the western part of the domain (see Fig. 6).

#### 4.4. Numerical results: validation and discussion

As mentioned previously, the analytical solutions used to test the transport components require steady-state and uniform flow conditions over the entire domain. In order to make sure that we achieve these conditions in the benchmark problem defined in Section 4.1, we first test whether the model can reproduce the desired flow field.

##### 4.4.1. Groundwater transport

Fig. 7 shows the steady-state potentiometric heads simulated by the GW flow component for the scenario "S1".

The results show a uniform, steady-state and unidirectional pressure gradient, which leads to the development, as designed (see Section 4.3), of a steady-state seepage velocity of 1/3 m s<sup>-1</sup>.

Fig. 8 compares the numerical results of the GW transport component with the corresponding analytical solution at two different time instants.

The model results agree quite well with the analytical solution over the entire domain. The small discrepancies observed are caused by numerical dispersion and their magnitude is below the acceptable absolute error suggested for the standalone version of MT3DMS by the developers manual (Zheng and Wang, 1999).

##### 4.4.2. Surface water transport

Fig. 9 shows water level, velocity, shear velocity, turbulent viscosity and diffusivity distributions after reaching steady-state flow

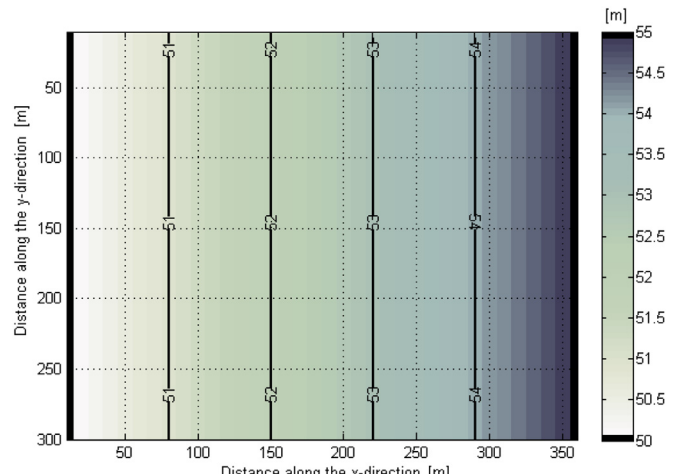
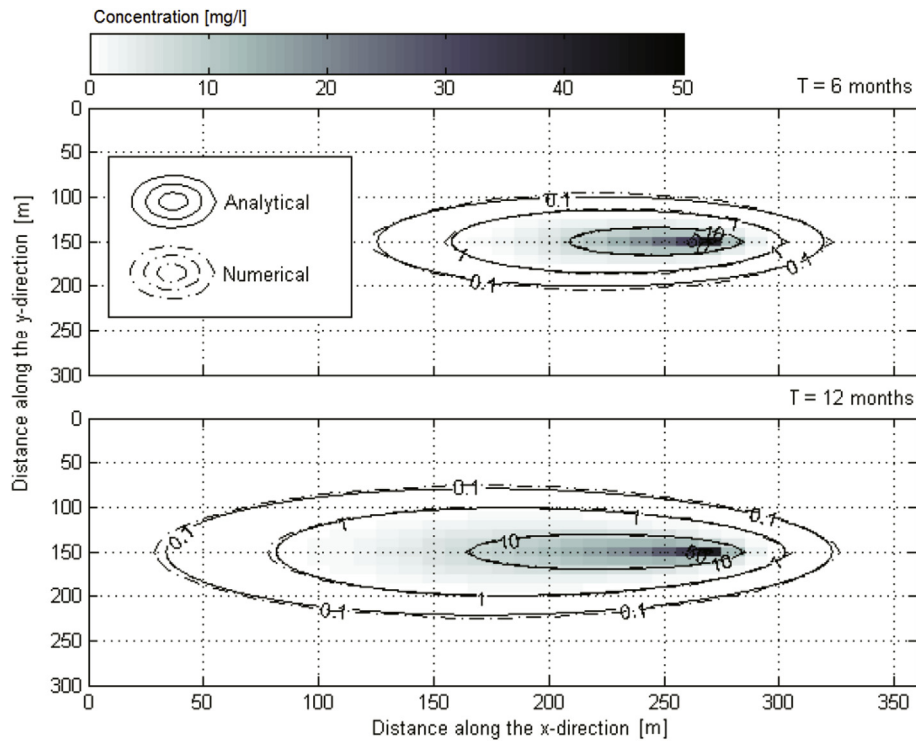
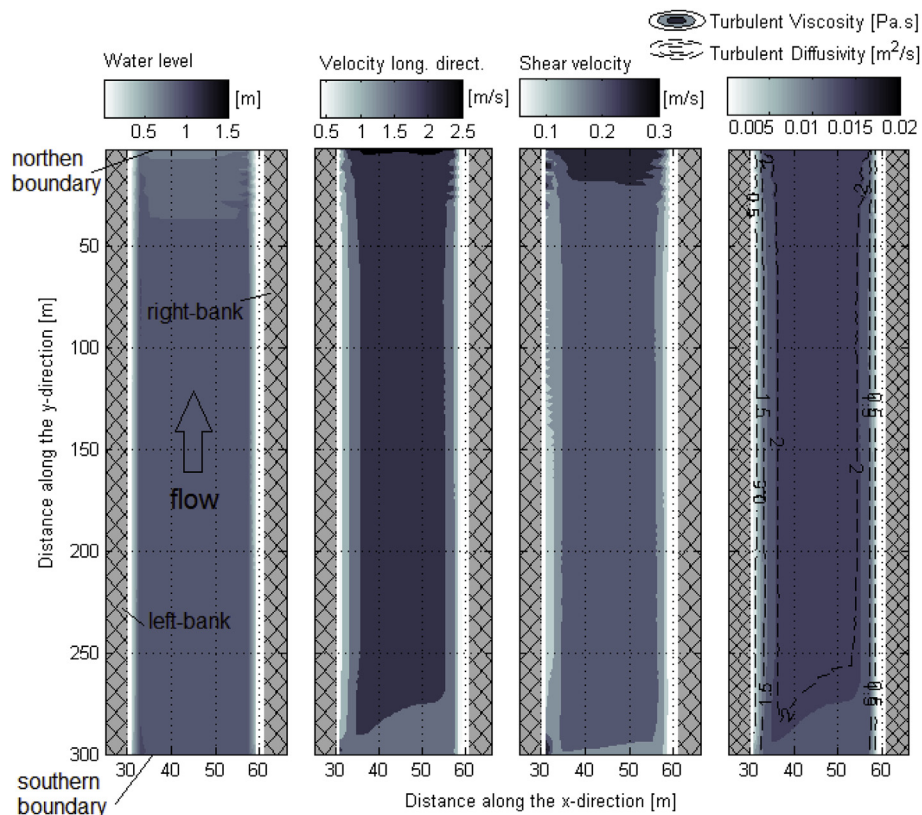


Fig. 7. Potentiometric heads ( $\psi$ ) simulated by the groundwater flow component.



**Fig. 8.** Comparison between analytical and numerical solutions at two different instants, 6 months and 12 months.



**Fig. 9.** Numerical results obtained with the SW flow component for water level ( $\xi$ ), velocity in the longitudinal direction ( $v$ ), shear velocity ( $u^*$ ), turbulent viscosity ( $\nu_t$ ) and turbulent diffusivity ( $E_H^{turb}$ ).

conditions in scenario "S1".

Steady state conditions are well approximated with only minor deviations which, however, deserve some considerations. As expected, due to the finite size of the domain, results show that velocities are smaller near the river banks because of friction. The effect of boundary conditions at the northern and southern boundaries can also be observed. This causes the eddy diffusivity and eddy viscosity distributions, which affect the dispersive transport of solutes, to be also non-uniform in these areas.

However the domain of the benchmark problem allows to identify a sufficiently broad region, highlighted in Fig. 10, that is unaffected by non-uniform behaviours, where we can test the performance of the SW transport component against the analytical solution. Evidence of steady state for the selected region is provided in Fig. 10, where all flow-related variables are constant in the region, highlighted with shaded cross-lines. Only eddy diffusivity varies slightly along the flow direction, corresponding, however, to the value used in the analytical solution to the average,  $1.8 \text{ m}^2\text{s}^{-1}$ .

The comparison of the analytical and numerical solution of the transport component illustrated in Fig. 11 shows that the numerical model captures well the overall concentration distribution predicted by the analytical solution, both spatially and temporally. The small discrepancies are caused by the above mentioned variability of the driving flow variables simulated by the SW flow component and by the plume encountering the river banks in the numerical solution, effect which becomes more pronounced with time. The absolute errors in the comparable regions are yet still within an accepted range similar to that of the groundwater model component.

#### 4.4.3. River-groundwater interactions: flow and transport

As pointed out further above, there are no analytical solutions for the transport component of the conductance-based model. We therefore compare the results obtained with FLUXOS for the

scenario "S2" with those predicted by MODFLOW and MT3DMS standalone versions when externally coupled. This test case was indeed conceptualized in a way so that it could be also simulated with the standalone models: steady-state and uniform with fluxes occurring in one direction only. To this end, we combined the *River and Stream (RIV) Package* in MODFLOW with the *Source Sink Mixing (SSM) Package* in MT3DMS – see panel (a) in Fig. 12.

Because the *RIV Package* in MODFLOW uses the conductance-based model approach in the form of the dominant clogging layer method as implemented in FLUXOS, in the externally coupled simulation, we used the same values of  $k_c$ ,  $b$  and  $\xi$  (see Eq. (8)) used in FLUXOS (see Table 1). Regarding the river water stage, it was set to 0.8546 m, which corresponds to the average value estimated for the entire model domain – see left panel in Fig. 9. MT3DMS was externally linked to MODFLOW using the *SSM Package*, which requires the definition of a constant loading rate. This was calculated as  $\approx 7.384 \text{ mg day}^{-1}$  using the infiltration rates determined by the standalone version of MODFLOW and the concentration fixed for the river (see simulation "S2" in Table 2).

Panel (b) in Fig. 12 shows the infiltration fluxes computed by FLUXOS as compared to those obtained with MODFLOW and MT3DMS standalone versions for scenario "S2".

The simulated infiltration fluxes are similar using both model approaches. The mismatch across predictions observed near the boundaries is the effect of boundary conditions in the surface flow and transport models, which was already discussed in Section 4.4.2.

## 5. Model applications

An early application of the model, which is documented in Costa et al. (2015), was carried out for the reach of the River Ciliwung crossing Bukit Duri ( $6^\circ 13' 17''\text{S}$   $106^\circ 51' 36''\text{E}$ ) in Kampung Melayu, an urban hamlet located in the heart of Jakarta, the South East Asian capital of Indonesia. This is an interesting test case, which we also

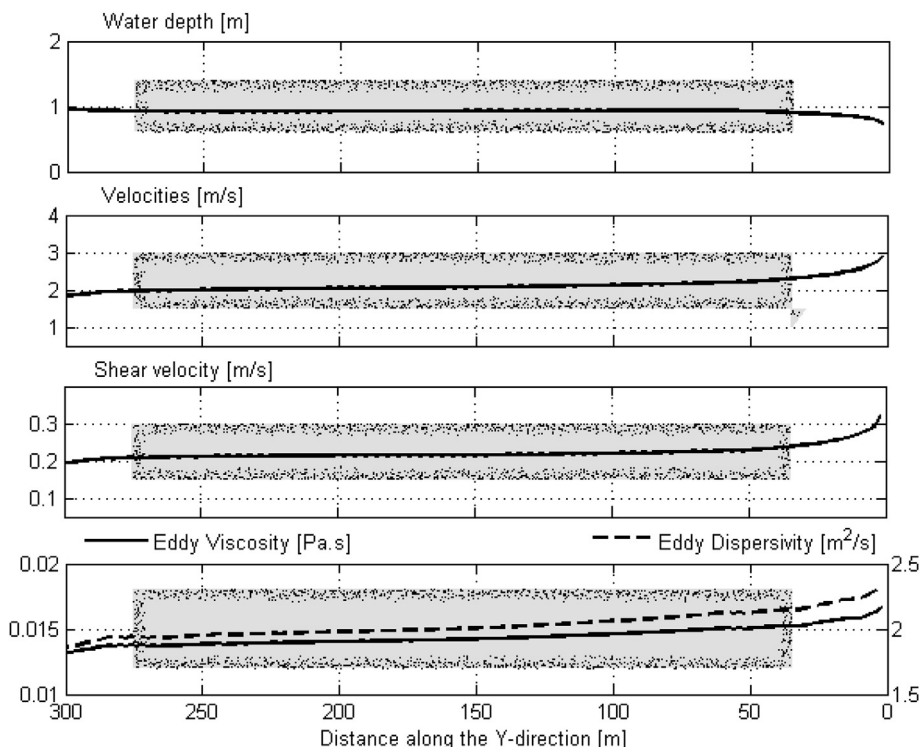


**Fig. 10.** Simulation results along the longitudinal transect following the river centreline for the SW component. The region highlighted in all panels (in grey with speckles) corresponds to the area suitable for comparison with the analytical solution.

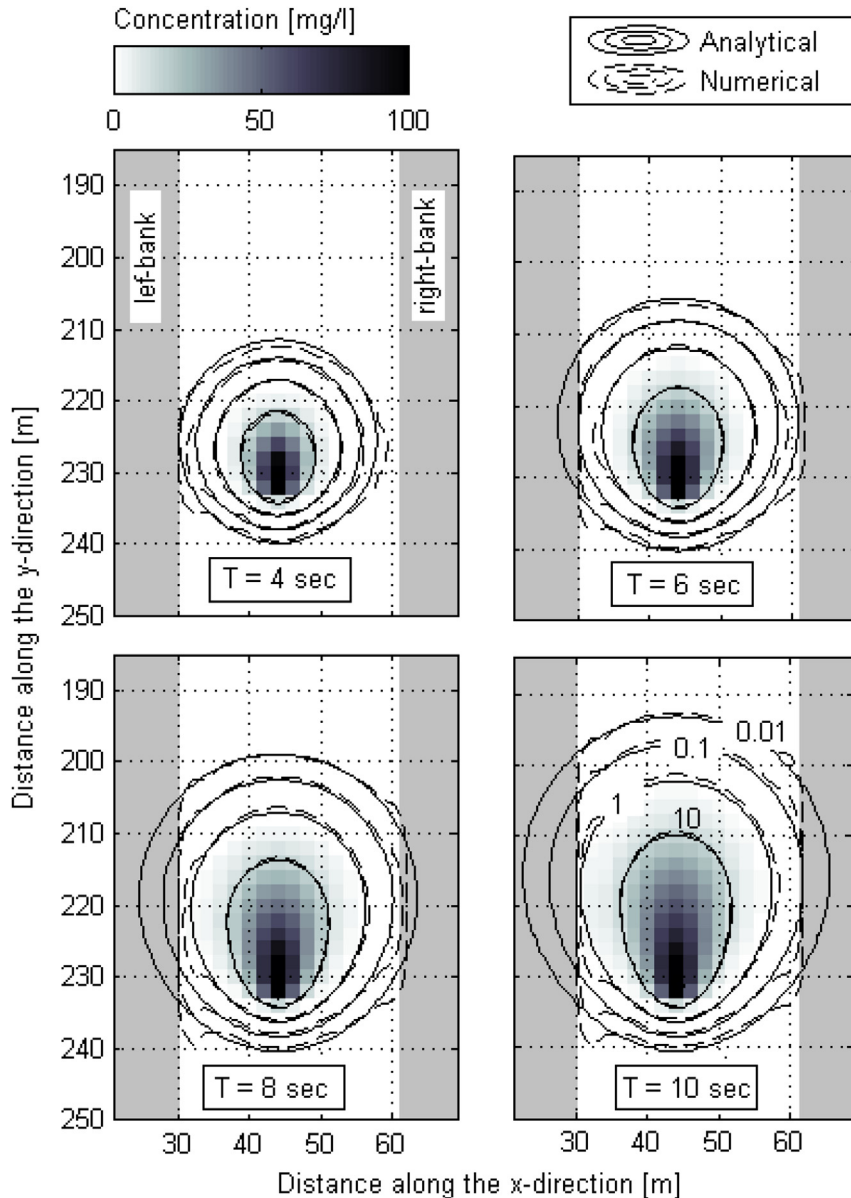


**Fig. 11.** Comparison between analytical and numerical solutions for the surface transport component.

use here, because of the multifaceted quantity and quality problems it presents, which can challenge the sensitivity of the model in relatively extreme environments, where design and management can better profit from simulation tools such as FLUXOS.

To further demonstrate the suitability of the model for cases beyond this application, as well as in relation to other prior practical applications which we have mentioned in Section 2, we tested the sensitivity of FLUXOS through a series of scenarios representative of real world cases that cannot be explicitly simulated by existing uncoupled or single-compartment state-of-the-art models.

### 5.1. The Ciliwung River

The metropolitan area of Jakarta is crossed by 13 rivers, the major being the Ciliwung River with a length of approximately 130 km. The shallow aquifer of Jakarta is 80 m depth and highly permeable (Fachri et al., 2003).

Management of water resources and river corridors in rapidly

growing cities like Jakarta typically involve complex interactions with the urban environment. The specific case of the Ciliwung River crossing Jakarta includes: The specific case of the Ciliwung river-aquifer system is particularly interesting and suitable to test FLUXOS because it involves:

1. Recurrent river flooding (e.g., Farid et al., 2012);
2. Pollution of surface and groundwater due to multiple untreated domestic and industrial wastewater discharges (e.g., Sinaulan et al., 2013);
3. Widely spread groundwater contamination caused by septic tanks leakages (e.g., Kagabu et al., 2013) and infiltration of polluted river flows;
4. General urban pollution, including solid waste, eventually reaching the Ciliwung transported by urban runoff and river flooding (e.g., Vollmer and Grét-Regamey, 2013); and
5. Alternating river-groundwater flow exchange directions which may arise, among other reasons, from the lowering of Jakarta's

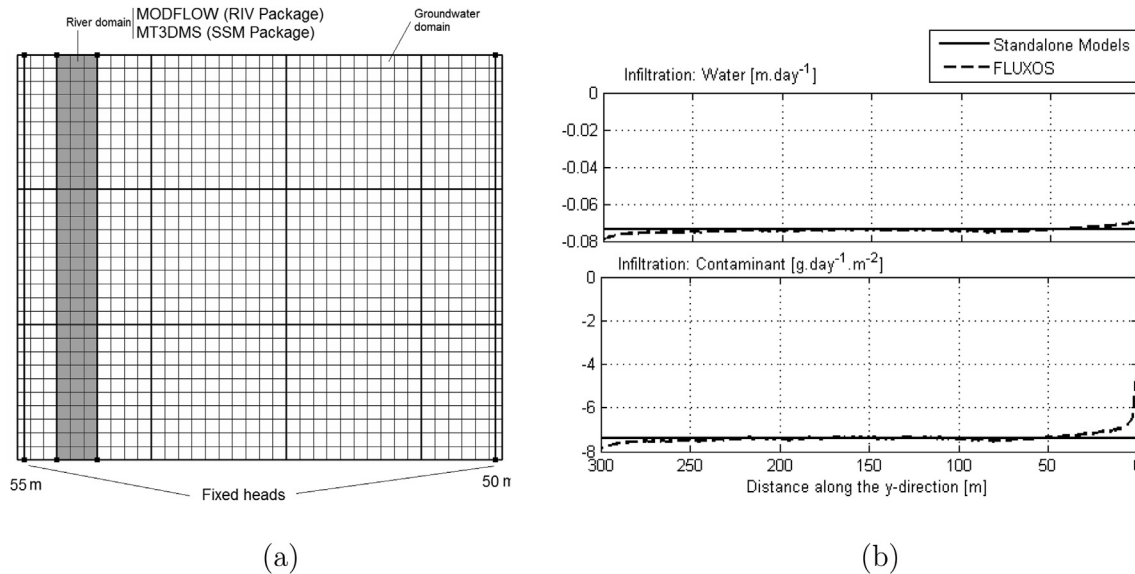


**Fig. 12.** (a) Setup of MODFLOW and MT3DMS standalone models. (b) Comparison between infiltration fluxes computed with the standalone models and FLUXOS.

water table, the effect of which has resulted in land subsidence and saline intrusion problems (e.g., [Oude Essink, 2001](#)), and from frequent flooding.

The few and sparse data available make this case study the ideal test bed to show the diagnostic and prognostic use of FLUXOS to investigate pollution sources and pathways, thus supporting the development of better informed rehabilitation strategies for urban river corridors.

### 5.2. Model and numerical experiment setup

The modelled region – shown in Fig. 13 – is approximately 9 ha in size ( $400 \times 220$  m). Point cloud (terrain) data was obtained for this region at a high resolution (11 cm) using stereo photography

techniques from images captured by a series of UAV (Unmanned Aerial Vehicle) campaigns ([Lin and Girot, 2014](#)), which, after processing, produced the geo-referenced DTM used in the numerical analysis (Fig. 13). To this purpose we used the cubic convolution algorithm ([Keys, 1981](#)), in order to upscale raw terrain data to 2 and 10 m horizontal resolution DTMs for use, respectively, with the river and groundwater models.

The detailed setup of each model component, which is summarized in Table 3, was kept the same for all the simulated scenarios. The parameters of the model are specific to the region and were used across all scenarios. However, some of them are non-site specific average values taken from the literature because they were not available for this region. A few parameters, finally, were fixed to different values to characterise each of the considered scenarios.

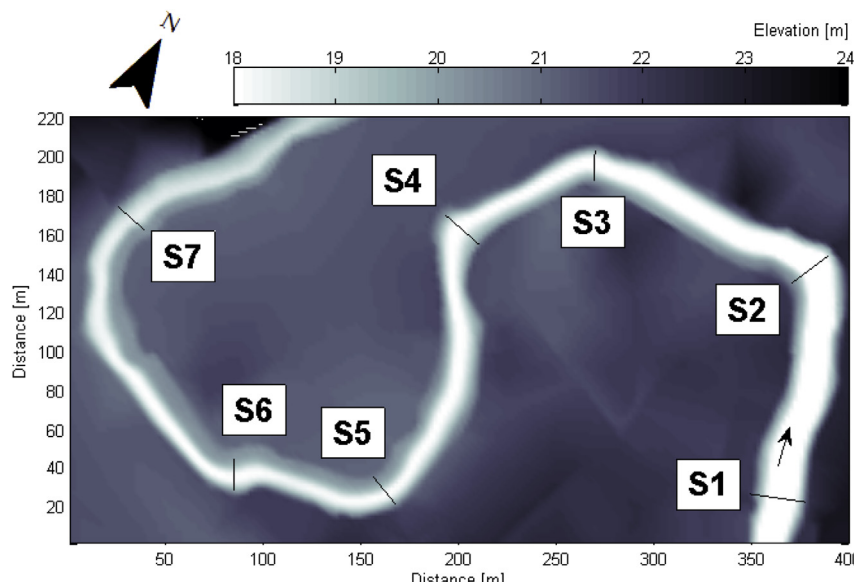


**Fig. 13.** DEM of the investigated site with cross-sections highlighted for reference with regard to the simulation results. The arrow shows the direction of the flow.

**Table 3**

General description of the model setup. The source of the data is marked with an (A) when it is specific to the test case region, with a (B) when it is an average or plausible value taken from the literature, and with a (C) when it has been chosen specifically for the purpose of the simulation. "IC" and "BC" refer to initial and boundary conditions.

Model component	Paramet. and Charac.	Value	Reference
GW flow	shallow aquifer type	unconfined	(A) (e.g., Hosono et al., 2011)
	aquifer thickness	80 m	(A) (Kagabu et al., 2013)
	flow direction	Northwards	(A) (Lubis et al., 2008)
	long. pressure grad.	$\frac{dh}{dx} = 0$	(A) (Lubis et al., 2008)
	trans. pressure grad.	$\frac{dh}{dy} = 2/3000$	(A) (Lubis et al., 2008)
	hydraulic conduct.	$K_{x,y} = 8.64 \text{ m day}^{-1}$	(A) (Djaeni et al., 1986)
SW flow	friction coefficient	0.13	(B)
k/l model	streambed conductance	$k_c = 1E-5 \text{ m s}^{-1}$	(B) (Brunke, 1999)
GW transport	porosity	0.3	(B)
	long. dispersivity	$\alpha_L = 10 \text{ m}$	(B)
	trans. dispersivity	$\alpha_T = 0.1\alpha_L$	(B)
	IC and BC	0 mg l <sup>-1</sup>	(C)
SW transport	IC and BC	3 mg l <sup>-1</sup>	(C)

### 5.3. Scenarios and model results

We considered two main groups of scenarios i.e. steady-state (SS) and transient (T), as summarized in Table 4. Both scenario groups were chosen to represent typical occurrences of interaction following uncontrolled and unplanned urban development along the river corridor which cannot be explicitly modelled by existing state-of-the-art models because they require the representation of hydraulic and water quality conditions that vary in space and, in some cases, also in time. More specifically, in the steady-state simulations we examine the capabilities of the model to address two different cases: one where a continuous pollution point load (e.g. industrial outfall) at a losing-stream (scenario "SS-CL") affects the groundwater, and one where a groundwater contaminated site (e.g. near an old petrol station) affects the quality of a nearby gaining-stream (scenario "SS-CS"). In the transient simulations we show how the coupled model can be used to investigate (1) the impact on groundwater of riverine flooding in polluted rivers on underlying aquifers (scenario "T-F-CL"), as it is the case of the Ciliwung in Central Jakarta, and (2) the impact of accidental spills in the river (scenario "T-IL"), which has been reported in different parts of the world (e.g. oil or uranium mill tailings spills, Wang et al., 2004) and have the potential to severely damage the quality of the water resources and endanger the affected communities.

The initial groundwater water depth was set to vary according to the north-south hydraulic gradient defined in Table 3 which was

fixed at -5 m and -5.14 m for respectively the northern and southern boundaries. In the particular case of the scenario "SS-CS", which involves exfiltration, the reference datum used to discuss the simulation results is the mean sea level to allow for more meaningful considerations and comparisons with the terrain elevation shown in Fig. 13 as the GW potentiometric heads rise above the terrain level.

The computational performance of FLUXOS depends not only on the size and spatial resolution of the SW and GW domains but also on the flow and transport regimes simulated (steady or unsteady). Model tests show also that the computational time is higher for gaining streams than for losing ones due to the number of cells involved in infiltration/exfiltration interactions increasing significantly. The reader is referred to the Supplementary Material for more information about the computational performance and resources of FLUXOS.

#### 5.3.1. Steady-state scenarios (SS)

5.3.1.1. *Losing-stream with point discharge (SS-CL).* Fig. 14 shows the simulation results for the river, interface and groundwater domains along the longitudinal transect cutting through the river centreline. The simulation was carried out for four independent cases (i.e. model run separately for each case), namely one baseline scenario for benchmarking, which does not consider any pollution loading point and is only affected by boundary and initial (contamination) conditions (BC and IC), denoted as scenario "SS-CL-No-load", and three other scenarios which, additionally to BC and IC, consider pollution loading points at S1, S3 and S5 cross-sections, denoted respectively as scenarios "SS-CL-S1", "SS-CL-S3" and "SS-CL-S5". For convenience, all scenarios are displayed in the same figure but they were all simulated independently. The "SS-CL-No-load" scenario is used to differentiate the effect of the pollution points, considered in the remaining scenarios, from that of boundary and initial conditions.

As expected, the spreading of the plume and the peak concentration in the river (left-axis, river-panel) depend on the hydrodynamic conditions. In fact, the concentration at the pollution loading point is the highest for the "SS-CL-S5" scenario because the water levels (right-axis, river-panel), and subsequently the dilution capacity, are the lowest. This makes the infiltration of pollutant into the groundwater highly heterogeneous. The total mass migrating to the underground water system depends also on the river-groundwater pressure gradient which, in the case of a losing-stream, is determined by the river water level. Therefore the location of the pollution loading point in relation to the flow conditions plays an important role in assessing the hazard level of aquifer contamination. The determination of the location of the most

**Table 4**

Characteristics of the scenarios considered, where "SS" and "T" refer to whether the simulation is steady-state or transient and "CL", "IL" and "CS" regards to the type of pollution scheme used, namely referring to continuous and instantaneous loading point source in the river and groundwater contamination site.

Location	Forcing type	Simulation ID			
		Steady-state (SS)		Transient (T)	
		SS-CL	SS-CS	T-F-CL	T-IL
River	Flow [m <sup>3</sup> /s]	3	3	20	3
River	CL in [g/s]	100	—	100	—
River	IL in [Kg]	—	—	—	100
GW	CS [Kg/year]	—	315	—	—
Contamination pathway					
Infiltration	X	X	X	X	
Exfiltration		X			
Contamination distribution <sup>a</sup>					
Heterogeneous	X	X	X	X	
Transient			X	X	

<sup>a</sup> The aim is to show cases which may produce non-linear flux distribution patterns that cannot be captured by current state-of-the-art models.

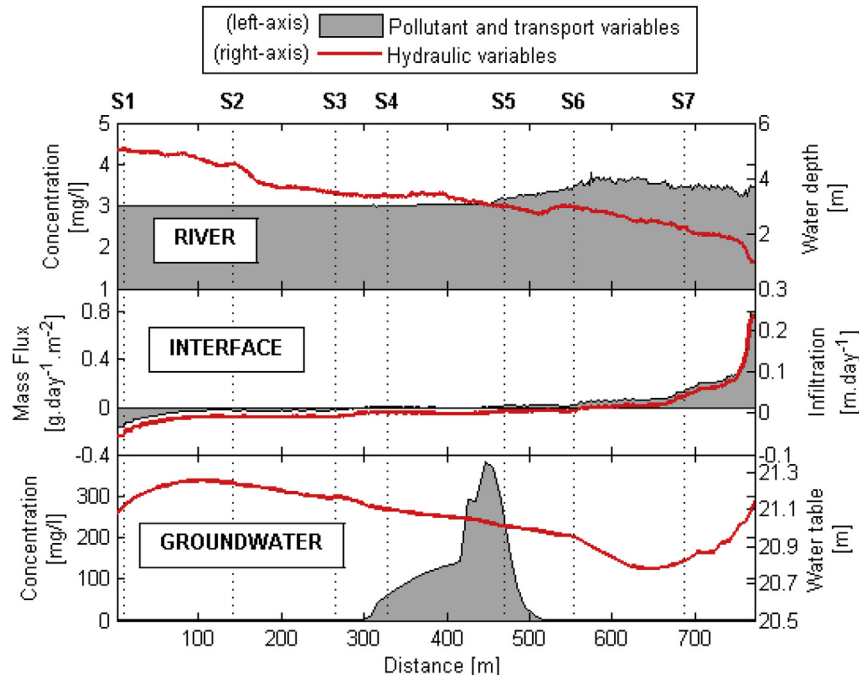


**Fig. 14.** Simulation results along the longitudinal transect following the river centreline for the SS-CL-No-load and three other scenarios, SS-CL-S1, SS-CL-S3 and SS-CL-S5. The pollution loading point is located for the three scenarios respectively at S1, S3 and S5. The solid (red) line refers to the hydraulic variables indicated on the right axes, whereas the shaded areas refer to the water quality variables indicated on the left axes. The dashed vertical lines correspond to the location of S1–S7 cross-sections. (For interpretation of the references to colour in this figure legend, the reader is referred to the web version of this article.)

hazardous conditions is thus best addressed using a framework like that of FLUXOS because, contrary to other models, it considers explicitly the temporal and spatial evolution of the plumes in both the river and aquifer and allows taking that into account in the simulation of exchange phenomena, which may aggravate (or respectively dampen) the effect of a pollution load.

It should be noted that the values depicted in Fig. 14 refer to simulation results along the centreline of the river and, therefore, the apparent drop in concentration, for instance between location S5 and S6 in scenario "SS-CL-S5", is due to the 2D diffusion and dispersion patterns (Fig. 15) that influence the plume concentration in the river centre trajectory.

In all simulations groundwater concentrations appear to be damped in comparison with those in the river. This effect is, however, a consequence of the grid resolution used for the groundwater domain, which was five times coarser than the river one to improve computational efficiency. In FLUXOS, like in any other grid-based model, the values computed for each grid cell correspond to the average value of the represented region. In this case, the river domain is discretised using  $2 \times 2$  meters grid cells to obtain a more detailed distribution of contaminants in the river, however the grid cells in the groundwater domain are set 5 times coarser ( $10 \times 10$  meters) and therefore represents the average of a much larger area. As a results, although the computed river-aquifer

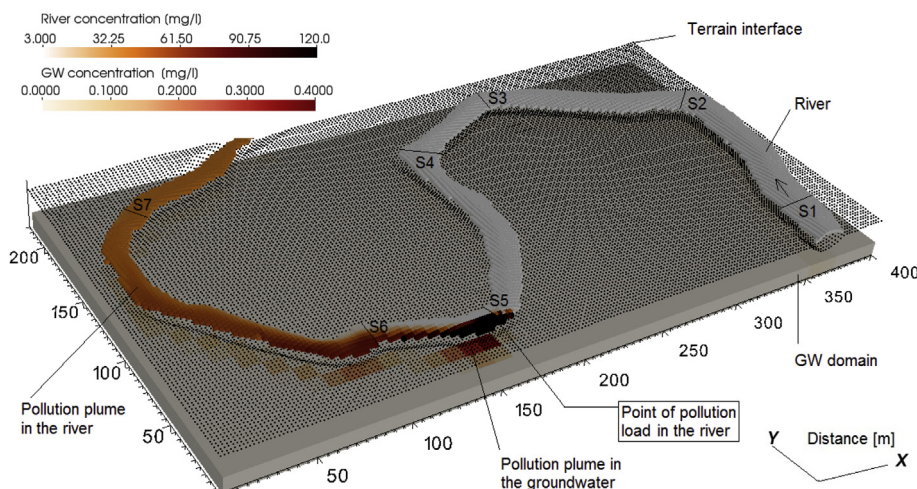


**Fig. 15.** Concentration distributions in the river and groundwater for scenario "SS-CL-S5". Location S5 (pollution load point) and S6 are marked to highlight that between these points the plume is not transported through the centre of the channel.

fluxes are particularly high at some river cells near the contamination points, its impact on the underlying groundwater top cells apparently seems somewhat damped, but this is due to the value in corresponding GW cell representing the average over a larger area. In other words, although the computation of both flow and contaminant exchanges between the SW and GW domains is not grid-dependent, it is so the resolution of the model outputs for each domain. This suggest that, despite the unquestionably higher realism of the results obtained from the joint simulation of flow and transport process in the river and aquifer, the choice of the domain resolution plays a crucial role with respect to compromising between computational demand and detailed representation of the investigated interaction phenomena. We observe also that the head gradient between the groundwater and river decreased along the centreline of the river longitudinal transect, x-axis, thus determining less water and pollutant entering the aquifer systems. This effect is visible for all scenarios in Fig. 14 from the inverse relationship between concentration (left-axis, Groundwater panel) and water table (right-axis, Groundwater panel). The hydraulic conditions of the GW system itself may also affect significantly the impact of contamination from the river as dilution arising from higher groundwater water columns may buffer river to groundwater contamination fluxes.

#### 5.3.1.2. Gaining-stream with aquifer contamination site (SS-CS).

The simulation of the “SS-CS” scenario consists of a continuous contamination load located at the coordinates (175, 175) of the domain (see Fig. 6).

The heterogeneous effect of polluted groundwater to river exfiltration shown in Fig. 16 is evident both (i) from the river flow, which increases significantly downstream of the exfiltration point (inferred from the extended river flow widths when compared to the case in Fig. 15) that in this case even causes flooding in some parts of the domain, and (ii) from the water quality, with pollutant concentrations in the river increasing when passing through the groundwater plume.

Fig. 17 shows the simulation results for the river, interface and groundwater domains along the longitudinal transect cutting through the river centreline and reveals that groundwater contamination affects the river water quality downstream S5 (left-axis, river-panel) due to exfiltration (flow and mass) only occurring in this region (interface-panel). In this particular scenario which involves both infiltration and exfiltration, the reference datum used

for the groundwater table is the sea level to make easier the comparison with the terrain elevation provided in Fig. 13.

Conversely, upstream of S5, infiltration is observed, which in this case translates in the transfer of pollutant from the river to the groundwater. However, no detectable impact in the groundwater concentration is observed due to the fluxes being small when compared to those caused by the main plume between S3 and S6 (groundwater panel, left-axis).

Moreover, results show that the interaction between river and groundwater is characterised by complex dynamics and non-linear feedback processes, which result in highly heterogeneous contaminant distributions due to high variability in space of the contaminant paths. Simulating simultaneously flow and transport in both the river and groundwater, as performed by FLUXOS, is therefore essential to capture and study such phenomena.

#### 5.3.2. Transient scenarios (T)

**5.3.2.1. Flooding of a losing stream with a continuous point discharge (T-F-CL).** The scenario “T-F-CL” tests the capability of the model to simulate hydraulic and water quality conditions that are both transient. Therefore, contrary to the previous cases where results were shown along the river path, panel (a) in Fig. 18 shows results over time, for the entire duration of the event, at three locations S1, S3 and S5. Relevant time instants in the simulation are highlighted: T1 and T2 are the spin-up times of the river flow and transport models and T3-T4 the period in which flow increases from 3 to 20 m<sup>3</sup>/s. In panel (b), the simulated river-aquifer fluxes are integrated across the model domain to allow quantifying the total effect of the transient regime.

In panel (a), it can be noted that, despite the gradual increase of infiltration after T3 (right-axis, interface-panel) – caused by higher river water levels (right-axis, river-panel) – the river to groundwater mass flux decreases instead (left-axis, interface-panel), because the concentration of pollutant in the river drops substantially (left-axis, river-panel) as a consequence of higher flow and dilution. This highlights, for this particular case, the temporary but dominant and positive effect of dilution that may reduce the contamination of the groundwater (left-axis, groundwater-panel), effect which cannot be captured by other models. Compared to simpler and single-compartment models, FLUXOS allows to simulate complex transient phenomena in which flow and water quality are highly dynamic in both the river and aquifer, and may lead to enhanced or damped system response. The effect of this

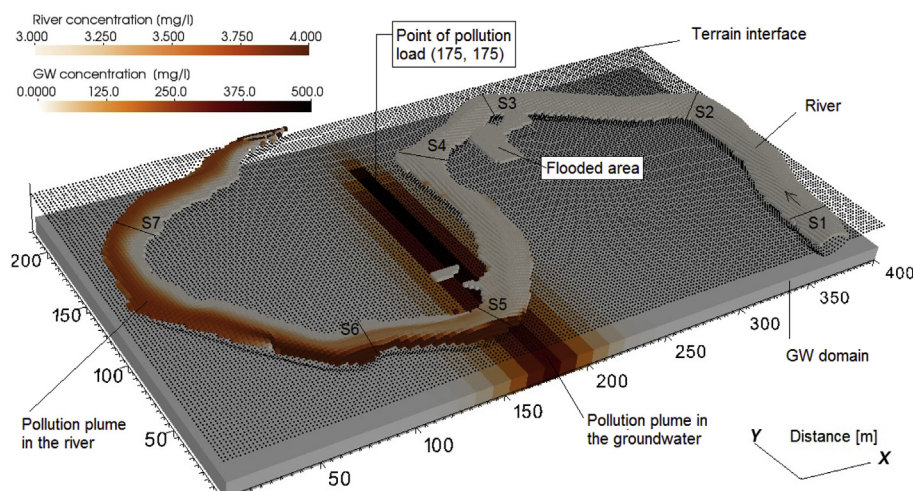
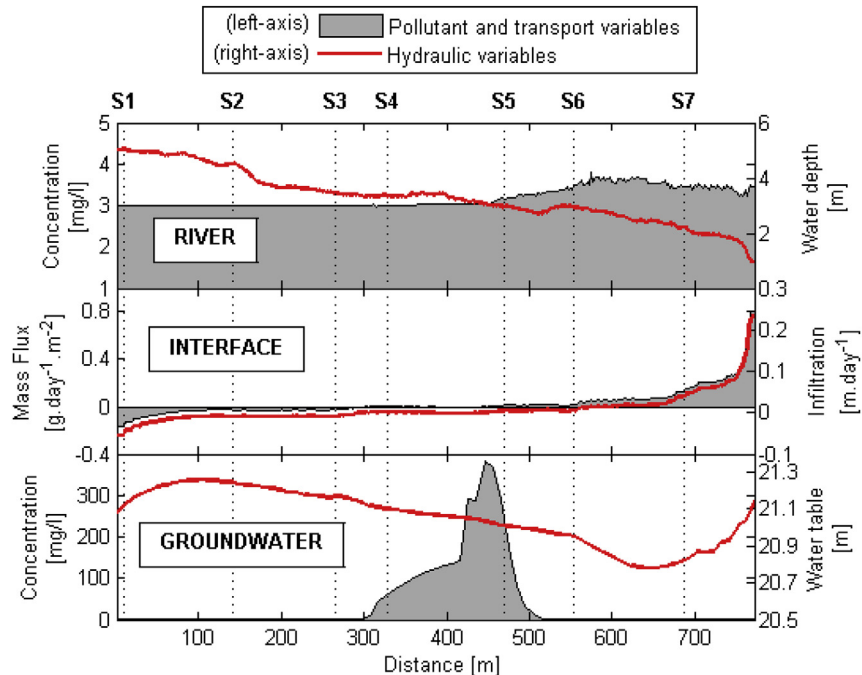


Fig. 16. Concentration distribution in the river and groundwater domains resulting for scenario “SS-CS”.



**Fig. 17.** Simulation results along the longitudinal transect following the river centreline for scenario "SS-CS". The solid (red) line refers to the hydraulic variables indicated on the right axes, whereas the shaded areas refer to the water quality variables indicated on the left axes. The dashed vertical lines correspond to the location of S1–S7 cross-sections. (For interpretation of the references to colour in this figure legend, the reader is referred to the web version of this article.)

transient behavior is relevant at localized scales as it is illustrated well by panel (b), which shows the total infiltration and mass-flux throughout the simulation for the entire domain.

The plot reveals that infiltration is approximately 4 times higher after T5 (right-axis) whereas the corresponding infiltration of pollutant mass is substantially reduced to nearly half of the initial rates (left-axis). This is the typical case where the complexity of FLUXOS is fully justifiable since the way the two systems interact is significantly affected by the heterogeneous and non-stationary hydraulic and water quality conditions of the river.

**5.3.2.2. Instantaneous spill in a losing stream (T-IL).** The simulation of scenario "T-IL" consists of the instantaneous release of a given contaminant load at the river location S1 and at time T1 in a losing stream. The river discharge was set constant at the upper boundary condition, whereas the transient regime concerns the water quality through the change of the contaminant concentration and the flow rate downstream of the upper section due to the losing character of the stream.

Panel (a) in Fig. 19 shows the simulation results for the river, interface and groundwater domains along the longitudinal transect cutting through the river centreline for instants T1, T2, T3 and T4, where T1 and T2 are the time steps immediately before and after the spill, and T3-T4 are the time steps at equally spaced intervals thereafter. As for the previous scenario, panel (b) shows the total infiltration and mass-flux rates to analyse the relevance of the event characterised in "T-IL" across the entire model domain.

From panel (a), one can note that the river to groundwater contamination rate (left-axis, interface-panel) is, as expected, strongly affected by the distribution over time of contaminant in the river (T2 to T4 shaded areas, left-axis, river-panel). The water levels slowly decreasing between S1 and S7 (right-axis, river-panel) induce a significant decrease of the groundwater contamination rate levels in the downstream reaches in comparison with those upstream (left-axis, interface-panel). As a consequence, higher

groundwater pollution levels occur in the upstream part (left-axis, groundwater panel). While intuitive, these results underline how the FLUXOS model, which can simulate the river-aquifer interaction dynamics explicitly across space and time, allows to quantify accurately the propagation dynamics of the polluting load throughout the aquifer in relation to changing flow conditions. This capability, which is not found on other state-of-the-art models, can be conveniently used to explore for instance scenarios of management strategies to mitigate the consequences of accident spills in rivers - phenomena which are transient and heterogeneous by nature - not only in the river itself, as typically is the case, but also on the quality of the groundwater.

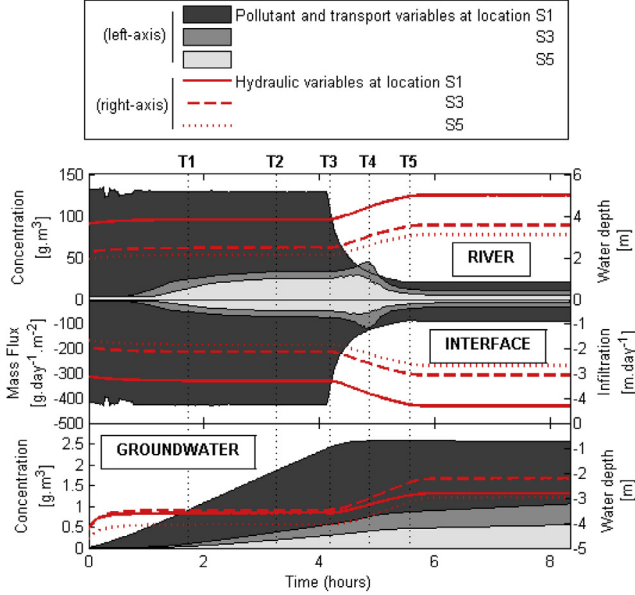
In panel (b), results show that the total contamination fluxes across the entire model domain increase by 15% between T1 and T2 (left-axis), which corresponds to the instants immediately after the release of the contaminant. As the plume moves with the flow and disperses, the rate of contamination gradually decreases, the effect of the spill being however still observed, in this particular case, more than 4 h after the release.

As for the previous case scenario "T-F-CL", these results also demonstrate that transient river quality conditions may have a temporary impact on the magnitude of the exchange fluxes between rivers and groundwater, effect which cannot be simulated by other models. Evidence from past incidents involving accident spills in rivers corroborate these model outcomes in that the effect on the quality of the groundwater can be significant at both local – panel (a) – and larger – panel (b) – scales (e.g. Santos et al., 2002; Graf, 1990), thus highlighting the need for more complete river-aquifer model frameworks, like that of FLUXOS, to address these particularly complex situations.

## 6. Conclusions

A new modelling framework, FLUXOS, which fully couples state-of-the-art standalone codes to model transport processes in river

(a) Simulation results at locations S1, S3 and S5



(b) Simulated river-aquifer fluxes integrated across the domain

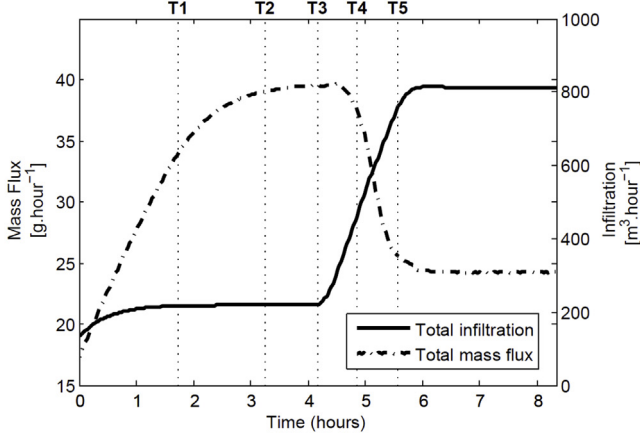
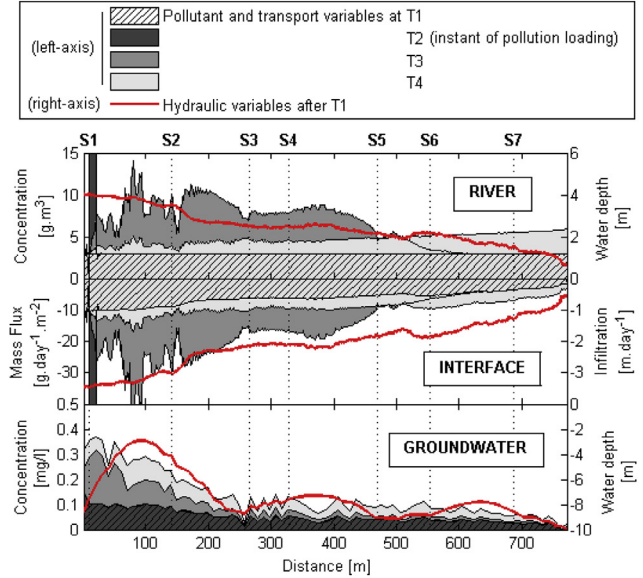


**Fig. 18.** (a) Transient scenario “T-F-CL” simulation results at the centre of different cross-sections (S1, S3 and S5) during the flood event. (b) Total infiltration (right y-axis) and mass-flux (left y-axis) for the entire model domain.

and groundwater systems with an integrated river-groundwater flow tool, was presented. The model was developed to overcome the limitations of existing single-system modelling approaches and catchment-scale hydrological models to provide accurate representations of complex phenomena that are controlled by the interaction between rivers and aquifers in highly dynamic river corridors, particularly in urban environments. Early applications of this new model showed that it is capable of providing a more accurate simulation of pollution pathways in connected river-aquifer systems when compared to results provided by existing single-system models, thus providing, in the context of the current paradigm of rapid urban development, an advanced and flexible tool both to investigate the effects of existing pollution and to plan management strategies that account for interacting surface and groundwater.

These capabilities are particularly relevant when river-groundwater interactions are extremely dynamic and involve complex non-linear feedback processes, which depend on the

(a) Simulation results at instants T1, T2, T3 and T4



(b) Simulated river-aquifer fluxes integrated across the domain

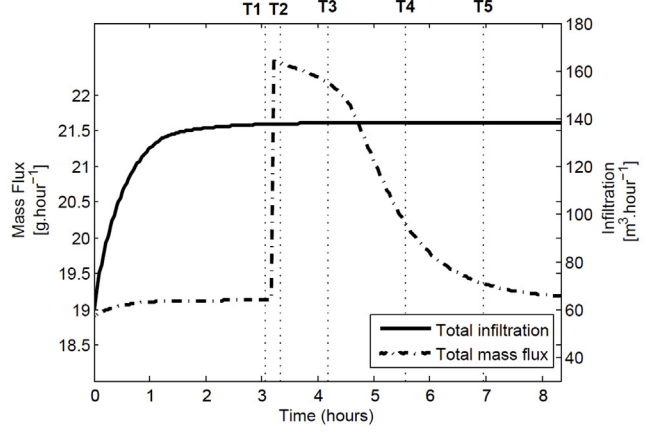


**Fig. 19.** (a) Simulation results along the longitudinal transect following the river centreline for scenario “T-IL” at instants T1, T2, T3 and T4. The dashed vertical lines correspond to the location of S1–S7 cross-sections. (b) Total infiltration (right y-axis) and mass-flux (dashed line, left y-axis) for the entire model domain.

spatial and temporal variability of vertical pressure gradients. These conditions occur typically between adjacent cells at the river-aquifer interface both in the case of infiltrating rivers and exfiltrating aquifers, and may have a significant influence on the distribution of pollutant concentrations.

Simulation results show that the exchange of flow and mass between the two systems was highly heterogeneous in all scenarios and varied significantly over time in the transient cases. The flux distribution patterns were strongly influenced by the hydraulic and water quality conditions, which caused different contamination levels along the river and affected both systems, demonstrating, on the one hand, the need for a model framework like that of FLUXOS to address such rather complex cases and, on the other hand, its effectiveness in investigating pollution pathways and in identifying vulnerable areas towards the definition of protection zones.

While the advancements of simulation capabilities provided by FLUXOS is evident from the presented results, further research is needed to achieve model developments that allow to overcome some of the limitations of the current model. First, to the

availability of more (experimental) data is key to further validate and progress the model. It is also important to enhance the computational efficiency by further rearranging parts of the code for parallel processing. Furthermore, additional packages need to be developed to account for other phenomena that are particularly important in environments where, for instance, (1) the hyporheic zone plays an important role for transport processes, (2) turbulence in river flow affects the dispersion of contaminants or (3) the reactions within a group of chemicals (e.g. nitrogen cycle) or in the benthic layer are important to predict the fate of the contaminant simulated.

Despite some limitations of the present version of FLUXOS, we are persuaded that this model represents an important step towards solutions for effective prevention and rehabilitation strategies in rapidly changing systems, such as those of urban rivers, which require an improved understanding of the complex interactions among hydrological, hydraulic and biochemical processes that occurs across the river-aquifer interface.

## Acknowledgments

The authors would like to thank the Singapore National Research Foundation (NRF) and the Singapore-ETH Centre (SEC) for the financial support. We would like to extend our gratitude to Kashif Shaad for developing and making available the coupling between 2dMb and MODFLOW, which was used as the basis for developing FLUXOS.

## Appendix A. Supplementary data

Supplementary data related to this article can be found at <http://dx.doi.org/10.1016/j.envsoft.2016.09.009>.

## References

- Abramowitz, M., Stegun, I.A., 2012. Handbook of Mathematical Functions: with Formulas, Graphs, and Mathematical Tables. Courier Dover Publications.
- Bear, J., 1979. Hydraulics of Groundwater, p. 569.
- Borsi, I., Rossetto, R., Schifani, C., Hill, M.C., 2013. Modeling unsaturated zone flow and runoff processes by integrating modflow-lgr and vsf, and creating the new cfl package. *J. Hydrol.* 488, 33–47.
- Brown, L.C., Barnwell, T.O., 1987. The Enhanced Stream Water Quality Models QUAL2E and QUAL2E-UNCAS: Documentation and User Manual. US Environmental Protection Agency. Office of Research and Development. Environmental Research Laboratory.
- Brunke, M., 1999. Colmation and depth filtration within streambeds: retention of particles in hyporheic interstices. *Int. Rev. Hydrobiol.* 84 (2), 99–117.
- Brunner, P., Simmons, C.T., 2012. Hydrogeosphere: a fully integrated, physically based hydrological model. *Ground Water* 50 (2), 170–176.
- Burnett, R., Frind, E., 1987. Simulation of contaminant transport in three dimensions: 1. the alternating direction galerkin technique. *Water Resour. Res.* 23 (4), 683–694.
- Carey, G., Pardhanani, A., 1989. Multigrid solution and grid redistribution for convection-diffusion. *Int. J. Numer. Methods Eng.* 27 (3), 655–664.
- Chapra, S.C., 2008. Surface Water-quality Modeling. Waveland Press.
- Costa, D., Burlando, P., Lioung, S.-Y., 2015. A new modelling framework to simulate transport in highly unsteady river-groundwater systems. In: Proceedings of the 36th IAHR World Congress, ISBN 978-90-824846-0-1 (The Hague, Netherlands).
- Costa, D., Burlando, P., Priadi, C., 2016a. The importance of integrated solutions to flooding and water quality problems in the tropical megacity of Jakarta. *Sustain. Cities Soc.* 20, 199–209.
- Costa, D., Burlando, P., Priadi, C., Lioung, S.-Y., 2016b. The nitrogen cycle in highly urbanized tropical regions and the effect of river-aquifer interactions: the case of Jakarta and the Ciliwung River. *J. Contam. Hydrol.* 192, 87–100.
- Costa, D., Gurusamy, S., Burlando, P., Lioung, S.-Y., 2014. Modelling the impact of urban floods in heavy polluted river: the case of Kampung Melayu in Jakarta. In: Book of Proceedings of the 3rd IAHR Europe Congress. IAHR, Porto, Portugal, ISBN 978-989-96479-2-3.
- Courant, R., Friedrichs, K., Lewy, H., 1928. ber die partiellen differenzengleichungen der mathematischen physik. *Math. Ann.* 100 (1), 32–74. <http://dx.doi.org/10.1007/BF01448839>.
- Djaeni, A., Hobler, M., Schmidt, G., Soekardi, P., Soefner, P., 1986. Hydrogeological investigations in the greater Jakarta area/Indonesia. In: Paper for Presentation in the Ninth Salt Water Intrusion Meeting, Delft.
- Fachri, M., Djauhaeni, H.L., Ramdhana, A., 2003. Stratigraphy and hydrostratigraphy in Jakarta groundwater basin. *Bull. Geol. Bdg. Instit. Technol.* 34 (3), 169–189.
- Fäh, R., 1997. Numerische simulation instationärer freispiegel-abflüsse, mit berücksichtigung der wechselwirkung von strömung, sedimenttransport und gerinnemorphologie. Ph.D. thesis. Eidgenössische Technische Hochschule Zürich.
- Farid, M., Mano, A., Udo, K., 2012. Urban flood inundation model for high density building area. *J. Ref. J. Disaster Res.* 7 (5), 554–559.
- Furman, A., 2008. Modeling coupled surface–subsurface flow processes: a review. *Vadose Zone J.* 7 (2), 741–756.
- Gander, W., Gautschi, W., 2000. Adaptive quadraturerevisited. *BIT Numer. Math.* 40 (1), 84–101.
- Graf, W.L., 1990. Fluvial dynamics of thorium-230 in the church rock event, Puerco river, New Mexico. *Ann. Assoc. Am. Geogr.* 80 (3), 327–342.
- Haitjema, H., Kelson, V., Lange, W., 2001. Selecting modflow cell sizes for accurate flow fields. *Groundwater* 39 (6), 931–938.
- Hallegatte, S., Green, C., Nicholls, R.J., Corfee-Morlot, J., 2013. Future flood losses in major coastal cities. *Nat. Clim. Change* 3 (9), 802–806.
- Hanson, R.T., Boyce, S.E., Schmid, W., Hughes, J.D., Mehl, S.W., Leake, S.A., Maddock III, T., Niswonger, R.G., 2014. One-water Hydrologic Flow Model (modflow-owhm). Tech. rep.. US Geological Survey Survey Techniques and Methods 6-A51, p. 120. <http://dx.doi.org/10.3133/tm6A51>.
- Harbaugh, A.W., 2005. MODFLOW-2005, the US Geological Survey Modular Ground-water Model: the Ground-water Flow Process. US Department of the Interior, US Geological Survey.
- Harbaugh, A.W., Banta, E.R., Hill, M.C., McDonald, M.G., 2000. MODFLOW-2000, the US Geological Survey Modular Ground-water Model: User Guide to Modularization Concepts and the Ground-water Flow Process. US Geological Survey Reston, VA, USA.
- Heilig, G.K., 2012. World Urbanization Prospects: the 2011 Revision. United Nations, Department of Economic and Social Affairs (DESA), Population Division, Population Estimates and Projections Section, New York.
- Hosono, T., Nakano, T., Shimizu, Y., Onodera, S.-i., Taniguchi, M., 2011. Hydrogeological constraint on nitrate and arsenic contamination in asian metropolitan groundwater. *Hydrol. Process.* 25 (17), 2742–2754.
- Ivanov, V.Y., Vivoni, E.R., Bras, R.L., Entekhabi, D., 2004. Preserving high-resolution surface and rainfall data in operational-scale basin hydrology: a fully-distributed physically-based approach. *J. Hydrol.* 298 (1–4), 80–111. [www.scopus.com](http://www.scopus.com).
- Kagabu, M., Shimada, J., Delinom, R., Nakamura, T., Taniguchi, M., 2013. Groundwater age rejuvenation caused by excessive urban pumping in Jakarta area, Indonesia. *Hydrol. Process.* 27 (18), 2591–2604.
- Kalbus, E., Reinstorf, F., Schirmer, M., 2006. Measuring methods for groundwater–surface water interactions: a review. *Hydrol. Earth Syst. Sci. Discuss.* 10 (6), 873–887.
- Keys, R., 1981. Cubic convolution interpolation for digital image processing. *Acoust. Speech Signal Process. IEEE Trans.* 29 (6), 1153–1160.
- Langevin, C., Swain, E., Wolfert, M., 2005. Simulation of integrated surface-water/ground-water flow and salinity for a coastal wetland and adjacent estuary. *J. Hydrol.* 314 (1), 212–234.
- Lerner, D.N., 2002. Identifying and quantifying urban recharge: a review. *Hydrogeol. J.* 10 (1), 143–152.
- Lin, E., Girot, C., 2014. Point cloud Components Tools for the Representation of Large Scale Landscape Architectural Projects. Wichmann.
- Loague, K., Heppner, C.S., Mirus, B.B., Ebel, B.A., Ran, Q., Carr, A.E., Beville, S.H., VanderKwaak, J.E., 2006. Physics-based hydrologic-response simulation: Foundation for hydroecology and hydrogeomorphology. *Hydrol. Process.* 20 (5), 1231–1237.
- Lubis, R.F., Sakura, Y., Delinom, R., 2008. Groundwater recharge and discharge processes in the Jakarta groundwater basin, Indonesia. *Hydrogeol. J.* 16 (5), 927–938.
- Ma, L., He, C., Bian, H., Sheng, L., 2016. MIKE SHE modeling of ecohydrological processes: merits, applications, and challenges. *Ecol. Eng.* <http://dx.doi.org/10.1016/j.ecoleng.2016.01.008>.
- Mehl, S., Hill, M.C., 2010. Grid-size dependence of cauchy boundary conditions used to simulate stream–aquifer interactions. *Adv. Water Resour.* 33 (4), 430–442.
- Oude Essink, G.H., 2001. Improving fresh groundwater supply – problems and solutions. *Ocean Coast. Manag.* 44 (5), 429–449.
- Prommer, H., Barry, D., Zheng, C., 2003. Modflow/mt3dms-based reactive multi-component transport modeling. *Groundwater* 41 (2), 247–257.
- Rassam, D., Pagendam, D., Hunter, H., 2008. Conceptualisation and application of models for groundwatersurface water interactions and nitrate attenuation potential in riparian zones. *Environ. Model. Softw.* 23 (7), 859–875. <http://www.sciencedirect.com/science/article/pii/S1364815207002150>.
- Rassam, D.W., 2011. A conceptual framework for incorporating surfacegroundwater interactions into a river operationplanning model. *Environ. Model. Softw.* 26 (12), 1554–1567. <http://www.sciencedirect.com/science/article/pii/S1364815211001800>.
- Refsgaard, J., Storm, B., Singh, V., et al., 1995. Mike she. *Comput. Models Watershed Hydrol.* 809–846.
- Ruf, W., 2007. Numerical Modelling of Distributed River-aquifer Coupling in an Alpine Floodplain. Ph.D. thesis. Eidgenössische Technische Hochschule Zürich. Diss ETH 17534.
- Santos, A., Alonso, E., Callejon, M., Jimenez, J., 2002. Heavy metal content and speciation in groundwater of the guadamar river basin. *Chemosphere* 48 (3),

- 279–285.
- Shaad, K., 2015. Development of a Distributed Surface-subsurface Interaction Model for River Corridor Hydrodynamics. Ph.D. thesis #22600. Eidgenössische Technische Hochschule Zürich. <http://dx.doi.org/10.3929/ethz-a-010487236>.
- Shaad, K., Burlando, P., 2014. Investigating grid-size dependency in coupled surface-subsurface hydraulics. In: Proceedings of the International Conference on Fluvial Hydraulics. Lausanne.
- Sinaulan, J.H., Nuhfil Hanani, A.R., Tyasmoro, S.Y., Nugroho, B.A., 2013. Behaviour analysis of riverbank society on pollution of water quality in Ciliwung river downstream, Jakarta. *Dev. Ctry. Stud.* 3 (12), 16–24.
- Sophocleous, M., 2002. Interactions between groundwater and surface water: the state of the science. *Hydrogeol. J.* 10 (1), 52–67. <http://dx.doi.org/10.1007/s10040-001-0170-8>.
- Tian, Y., Zheng, Y., Wu, B., Wu, X., Liu, J., Zheng, C., 2015. Modeling surface water-groundwater interaction in arid and semi-arid regions with intensive agriculture. *Environ. Model. Softw.* 63, 170–184. <http://www.sciencedirect.com/science/article/pii/S1364815214003016>.
- Un-Habitat, 2008. State of the World's Cities 2008/9: Harmonious Cities. Earthscan.
- Vollmer, D., Grét-Regamey, A., 2013. Rivers as municipal infrastructure: demand for environmental services in informal settlements along an Indonesian river. *Glob. Environ. Change* 23 (6), 1542–1555.
- Wang, L., Wei, J., Huang, Y., Wang, G., Maqsood, I., 2011. Urban nonpoint source pollution buildup and washoff models for simulating storm runoff quality in the los angeles county. *Environ. Pollut.* 159 (7), 1932–1940.
- Wang, Z., Fingas, M., Lambert, P., Zeng, G., Yang, C., Hollebone, B., 2004. Characterization and identification of the detroit river mystery oil spill (2002). *J. Chromatogr. A* 1038 (1), 201–214.
- Wexler, E.J., 1992. Analytical Solutions for One-, Two-, and Three-dimensional Solute Transport in Ground-water Systems with Uniform Flow. US Government Printing Office.
- Winter, T.C., 1999. Ground Water and Surface Water: a Single Resource. US Geological Survey.
- Wong, V.N., Johnston, S.G., Bush, R.T., Sullivan, L.A., Clay, C., Burton, E.D., Slavich, P.G., 2010. Spatial and temporal changes in estuarine water quality during a post-flood hypoxic event. *Estuar. Coast. Shelf Sci.* 87 (1), 73–82.
- Zerihun, D., Furman, A., Warrick, A., Sanchez, C., 2005. Coupled surface-subsurface solute transport model for irrigation borders and basins. i. model development. *J. Irrig. Drain. Eng.* 131 (5), 396–406.
- Zheng, C., Wang, P.P., 1999. Mt3dms: a Modular Three-dimensional Multispecies Transport Model for Simulation of Advection, Dispersion, and Chemical Reactions of Contaminants in Groundwater Systems; Documentation and User's Guide. Tech. rep. DTIC Document.
- Zipperer, W.C., Pickett, S.T., 2012. Urban Ecology: Patterns of Population Growth and Ecological Effects. eLS.
- Zoppou, C., 2001. Review of urban storm water models. *Environ. Model. Softw.* 16 (3), 195–231.